69-15

EXPERIMENTAL MEASUREMENTS IN THE WAKE OF 10° HALF ANGLE BLUNTED AND POINTED CONES AT HYPERSONIC FLOW VELOCITIES

by

Samuel Lederman and Joel Avidor

MAY 1969

POLYTECHNIC INSTITUTE OF BROOKLYN

DEPARTMENT
of
AEROSPACE ENGINEERING
and
APPLIED MECHANICS

PIBAL REPORT NO. 69-15

sale; its distribution is unlimited.

51

EXPERIMENTAL MEASUREMENTS IN THE WAKE OF 10° HALF ANGLE BLUNTED AND POINTED CONES AT HYPERSONIC FLOW VELOCITIES

by

Samuel Lederman and Joel Avidor

This research has been conducted under Contract Nonr 839(38) for PROJECT STRATEGIC TECHNOLOGY, and was made possible by the support of the Advanced Research Projects Agency under Order No. 529 through the Office of Naval Research.

Polytechnic Institute of Brooklyn

Department

of

Aerospace Engineering and Applied Mechanics

May 1969

PIBAL Report No. 69-15

BLANK PAGE

EXPERIMENTAL MEASUREMENTS IN THE WAKE OF 10° HALF ANGLE BLUNTED AND POINTED CONES AT HYPERSONIC FLOW VELOCITIES[+]

by

Samuel Lederman[*] and Joel Avidor[**]

Polytechnic Institute of Brooklyn

ABSTRACT

Experimental measurements have been performed in the wake of a 10° half angle cone at 0° and 10° angle of attack with respect to the flow, and of a blunted cone of .333, and .666 bluntness ratio at 0° angle of attack. A rake of closely spaced (1" apart) electrostatic probes was utilized to obtain the relative electron density distribution at several stations behind the base of the cone. These electron densities can, under certain conditions and in most parts of the wake, be interpreted in terms of the neutral density distributions. It is concluded that the hypersonic shock tunnel in conjunction with simple electrostatic probes can, within limits, provide a good qualitative insight into the flow field of complex aerodynamic models.

[+] This research has been conducted under Contract Nonr 839(38) for PROJECT STRATEGIC TECHNOLOGY, and was made possible by the support of the Advanced Research Projects Agency under Order No. 529 through the Office of Naval Research.

[*] Associate Professor of Aerospace Engineering.

[**] Research Assistant

TABLE OF CONTENTS

LIST OF ILLUSTRATIONS

LIST OF ILLUSTRATIONS (Contd)

LIST OF ILLUSTRATIONS (Contd)

LIST OF ILLUSTRATIONS (Contd)

SECTION I

INTRODUCTION

The electron, as well as the neutral density distribution in the near wake and recirculation region of reentry type configurations has been receiving considerable attention. The interest in this aspect of wakes, apart from purely fluid-mechanical phenomena, is significantly related to the thermal ionization effects associated with reentry and the relevant problems of observation and communication. The electron density distribution in the wake is of particular interest in that respect. To obtain the latter, ground-based as well as in-flight measurements have been made[1-3]. The ground-based facilities utilized for the electron density measurements in the wake, in the above reference cited, were of the ballistic range type. In this work an attempt is being made to obtain the electron density distribution in the recirculation region and near wake region of a 10° half angle cone at 0° and 10° angle of attack with respect to the flow direction, and of blunted cones of .333 and .666 bluntness ratio at 0° angle of attack, utilizing the flow of a hypersonic pressure driven shock tunnel, operated at a density equivalent to about 250,000 ft. altitude. The free stream flow in these tests is slightly ionized and chemically frozen. The neutral and electron densities here are substantially higher than those in the ionosphere. Thus, although partial simulations relevant

to ionospheric flight disturbances could be attempted, this is not the purpose at present. The fluid dynamics associated with hypersonic flow at about 250 k ft. altitude is reasonably well-simulated here. Continuum effects dominate the flow over the present models. The correspondence between the neutral and electron density distribution in the flow field is, due to the chemically frozen conditions, maintained throughout, except possibly in the recirculation region where convection and diffusion effects are coupled and of comparable magnitude. Without entering into a lengthy discussion concerning the parameters which are simulated, it suffices to point out that a good qualitative insight into the flow field pattern can be obtained by this method as discussed in Ref. 4. As the diagnostic tool, a rake of negatively biased electrostatic probes was used. At this point the authors would like to express their appreciation to Dr. M.H. Bloom for stimulating and enlightening discussions and for his very valuable criticism and suggestions during the course of this work.

SECTION II

EXPERIMENTAL APPARATUS

The apparatus used in this research program was the hypersonic shock tunnel of the Polytechnic Institute of Brooklyn, located at the Graduate Center in Farmingdale. A detailed description of the facility and its performance capabilities are given in Refs. 5 and 6. The operating initial conditions of the shock tunnel were fixed

throughout this investigation. With an initial driven pressure of 38 m Hg air, and a driver pressure of 1800 psi Helium, a shock Mach number of about 7 was obtained. This resulted in a pressure of about 23 atmospheres and a temperature of about 3800°K behind the reflected shock. After expansion, the test chamber conditions were: Mach No. ~18, density ~$1.7.10^{-5}$ atm., mean free path about 6 mm. The free stream electron density was measured and found to be between $2\text{-}9(10)^{8}$ el/cm^3. When compared with the ambient neutral density of about $5(10)^{14}$ p/cm^3, this results in about <u>one</u> ionized particle in one million and can therefore, for all practical purposes, be neglected as far as its influence on the flow field is concerned. It can, however, in the context outlined in Ref. 4, be considered as a convenient tracer of the neutral density variation in non-diffusive regions since the flow is chemically frozen. The uniformity of the flow in the test section was determined[6] and found to occupy a central core of the test section of about 24". The models tested were a 10° half angle cone of 4" base diameter at 0° and 10° angle of attack, and a half angle cone of 6" base diameter of .333 and .666 bluntness ratio at 0° angle of attack. The models were suspended in the center of the test section by 0.020" wires. Flow field interference resulting from these supports could be considered negligibly small, since their dimensions are considerably less than the mean free path of the test gas.

As mentioned in the introductory remarks, the electrostatic probe was chosen as the diagnostic instrument. The choice of this type of a diagnostic tool was dictated by the desire to obtain pointwise, or near pointwise, electron or neutral density distribution in the wake and by the fact that this device is one of the simplest diagnostic tools, not only in terms of its construction, but also in terms of the necessary external circuitry for its use. Furthermore, it is suitable,in view of its simplicity and size, to be arranged in the form of a rake and thus permit the simultaneous acquisition of data at different stations.

Flow field considerations in the near wake, and particularly in the recirculation region, resulted in the design of an electrostatic probe rake configuration as seen in Fig. 1. The number density of the probes in the rake was limited not only by the desire to avoid interference of the probes with each other, but also by the requirement for the rake to be as small as possible in order to minimize the flow field disturbances. It must be kept in mind that each probe requires additional interconnecting cables with the resulting increases in rake size requirement. Therefore, in view of the known uniform test section flow core of about 24 inches at the exit of the conical nozzle, a rake equipped with 33 probes uniformly spaced at one inch between centers of the probes was designed. The construction of the rake was such that plug-in

type probes could be used.

In order to obtain better spacial resolution than that dictated by the one-inch spacing of the probes, the rake was moved back and forth one-half inch off-center in each alternate test to give an effective one-half inch spacial distribution, while minimizing the flow field interference. The probes used in this investigation had an effective length-to-diameter ratio of 50.

In all the tests the model remained stationary and the rake was moved. Tests were performed in the case of 0° angle of attack wherein the nondimensional distance of the rake behind the center of the model base to the diameter of the model, X/D, was varied from .25 to 4. In the case of the cone at 10° angle of attack, the cone was aligned with the flow direction parallel to one of the generating lines. A schematic diagram of the test section arrangement of the model and rake in the latter case is shown in Fig. 2. Included in this figure is a schematic diagram of the external circuit used to obtain the data from the electrostatic probes. The data, as indicated in the diagram, were recorded on Tektronix 565 oscilloscopes equipped with Polaroid cameras. In Fig. 2a, a schematic representation of the blunted cone is shown.

SECTION III

THE ELECTROSTATIC PROBE

The diagnostic tool used in this work is the biased cylindrical electrostatic probe used as an ion current collector operating under free molecular conditions. A collisionless theory applicable to such conditions has been detailed by Laframboise[7] and, for a cylindrical probe, can be expressed as follows:

for $X_p<0$

$$J_i = \frac{en}{4}\left(\frac{8kT_e}{\pi m_i}\right)^{\frac{1}{2}} \alpha_{p_i}\left(X_p; Rp/\lambda_D; \frac{T_i}{T_e}\right) \qquad (1)$$

$$J_e = \frac{en}{4}\left(\frac{8kT_e}{\pi m_e}\right)^{\frac{1}{2}} \exp X_p \qquad (2)$$

where T_i and T_e are the ion and electron temperature, respectively, $X_p = \frac{e(V-V_\infty)}{kT_e}$ is a dimensionless potential difference between the probe and plasma. The proportionality of the current density and the ion or electron number density is evident from the above equation. The proportionality factor, α_p, the so-called normalized nondimensional current, was calculated by Laframboise and presented in Ref. 7. As pointed out by Laframboise, and later confirmed by Sonin[8], this proportionality factor as obtained from the collisionless free molecular theory under the assumptions made was valid

only in the regime of $Rp/\lambda_D > 3$. Under certain conditions this restriction may be violated. In the case of the near wake, as will be seen later, the electron density may vary over a range of three orders of magnitude. This, in conjunction with the desirability of using as small a diameter wire as possible for the probe in order to minimize the flow field interference while keeping the length-to-diameter ratios large but finite, resulted in Rp/λ_D values much smaller than one. A knowledge of the behavior of this proportionality factor, α_p, for various L/D ratios, and $Rp/\lambda_D < 3$ is therefore necessary. Ref. 9 presents an experimental study of this parameter.

In Fig. 3, a plot of α_p as a function of Rp/λ_D is presented for the type of probes used herein, which is reproduced from Ref. 9. The collisionless free molecular theory as applied to cylindrical current collectors assumes, in the case of a flowing ionized gas, that the current collector is aligned with its axis parallel to the flow. Since, in the recirculation region of a near wake, this cannot always be the case, a knowledge of the effects of the angle of attack on the current collection is of importance. Fig. 4, reproduced here from Ref. 9, presents this effect. Since the theory of Laframboise is valid in the case of cylindrical probes only for infinitely long probes, the effect of finite length of the probes on current collection is of importance.

This was investigated in Ref. 9 and the conclusions are presented in Fig. 5. With these curves, Figs. 3, 4, and 5, the currents were reduced to electron densities.

SECTION IV

EXPERIMENTAL RESULTS

As pointed out above, a 4" base diameter 10^{o} half angle cone was tested in the course of this work. The model was suspended in the test section at zero and 10^{o} angle of attack. A schematic diagram of the test configuration is shown in Fig. 2. The rake of probes was mounted successively at a number of stations behind the model from X/D=.25 to X/D=4. With this type of configuration a number of tests were conducted. Fig. 6 presents a sample of the oscilloscope traces as obtained in these tests. Some of these traces show, after an initial peak, a relatively uniform time amplitude response, which can be considered the response of the probe to the established uniform flow. The data as obtained were analyzed utilizing both the peak values and the uniform flat response. As shown in Ref. 4, the qualitative behavior of the flow field could be obtained using either. In each case the data were normalized with respect to the free stream conditions. Thus the peak values in the wake were normalized to the free stream peak values, and the flat portions of the response in the wake, which

are indicative of the actual electron number densities, were normalized to the flat portions of the free stream probe responses.

Fig. 7 presents the normalized electron density distribution in the near wake of the 10° half angle cone with the rake located at X/D=.25. In this case the angle of attack of the cone with respect to the flow was 0°.

In Figs. 8 through 12, the normalized electron density distribution as a function of X/D from .25 to 3,with the model at an angle of attack of 10° with respect to the flow direction, is presented.

Fig. 13 shows a composite of the normalized electron number density with X/D as a parameter for the case of the cone at 0° angle of attack. Fig. 14 presents the same kind of composite for the case of the cone inclined 10° to the flow direction.

In Fig. 15, a composite of the radial distribution of the electron density in the wake of this cone at 0° and 10° angle of attack is shown at the two extreme stations, i.e., X/D=.25 and X/D=3.

Fig. 16 shows the experimental shock shape as obtained for the case of 0° angle of attack, and Fig. 17 presents the experimental shock shape for the case of the inclined cone.

Figs. 18 through 21 present the normalized electron density distribution in the wake of the blunted cone of .333 bluntness ratio at 0° angle of attack, while Figs. 22 through 25 present

the same distribution for the cone of .666 bluntness ratio. The shock shape obtained from these measurements are presented in Figs. 26 and 27 for the bluntness ratio of .333 and .666, respectively. As expected, the shock shapes in both cases are identical. A close inspection of the electron density distribution along the centerline of both blunted cones reveals a slightly lower density for the bluntness ratio of .333 than for .666. Although this feature appears to be consistent throughout the range of X/D measured, it is not possible at this point to draw any definite conclusions about this because of the limitations on accuracy imposed by some properties of the electrostatic probe method as, for example, the angle of attack of the probes.

A comparison of the radial electron density distribution of the blunted cones of different bluntness ratios with the cones of zero bluntness, as given in Figs. 18, 22, and 7, respectively, for the same X/D ratio, reveals a remarkable similarity in qualitative as well as quantitative distribution, although some minor quantitative differences do occur along the centerline distribution. There is an apparent decrease in the centerline electron density with the decrease in bluntness ratio. This may be due in some measure to some production of electrons at the stagnation point in the case of the blunted cones.

SECTION V

DISCUSSION OF RESULTS AND CONCLUSIONS

The relative electron density distribution in the near wake as presented above can, within limits, provide a qualitative insight into the flow field. As is evident from an inspection of any of the figures from 7 through 12, the overshoot of the electron density at the outer edges of the wake, its decrease in amplitude with its simultaneous increase of its distance from the axis as the distance of the rake from the base of the model increases, is an indication of the shock location. This feature is quite evident from Fig. 13, which is a superposition of the data obtained behind the cone at 0° angle of attack. The same feature, although to a lesser degree, emerges from Fig. 14, which represents a superposition of the electron density profiles behind the 10° half angle cone at a 10° angle of attack. This feature has been utilized in Figs. 16 and 17 to construct the shock location in the wake of the cone at 0° and 10° angle of attack, respectively, and in Figs. 26 and 27 to construct the shock shape behind the blunted cones of different bluntness ratio. A superposition of two of the extreme radial density distribution profiles,obtained in this work for both the 0° and 10° angle of attack of the cone to the flow direction, points out very clearly these features. The asymmetry in the wake distribution profiles is quite evident in comparison with the

profiles at 0^{o} angle of attack (Figs. 13 and 14). The same is true for the shock shape as evident from a comparison of Figs. 16 and 17.

It can, therefore, be concluded that a hypersonic shock tunnel in conjunction with simple electrostatic probes can provide a good insight into the flow field around complex aerodynamic models, providing almost pointwise electron density distributions which, under certain conditions, can be related to neutral density profiles.

SECTION VI

REFERENCES

1. Labitt, M.: The Measurement of Electron Density in the Wake of a Hypervelocity Pellet Over a Six-Magnitude Range. Massachusetts Institute of Technology, Lincoln Laboratories, Technical Report No. 307, April 1963.

2. Primrich, R.I., Hayanin, R.A., Auston, D.H., et al.: Free Flight Range Measurements of Ionization Behind Slender Hypersonic Velocity Cones. GM Defense Research Laboratory, Technical Report No. TR 65-19A, April 1965.

3. Kornegay, W.M.: Resonant Cavity Measurement of Ionized Wakes. Paper presented at the 2nd International Congress on Instrumentation in Aerospace Simulation Facilities, Stanford, Calif., August 1966.

4. Lederman, S., Bloom, M.H. and Widhopf, G.: Laboratory Measurements of Electron Density Distribution in the Near Wake. Polytechnic Institute of Brooklyn (in preparation).

5. Visich, M. Jr., Lederman, S. and Mak, W.H.: Combustion Driven Shock Tunnel of the Polytechnic Institute of Brooklyn. Polytechnic Institute of Brooklyn, PIBAL Report No. 847, January 1965.

6. Bloom, M.H. and Lederman, S.: Measurements of the Ionized Flow in a Shock Tunnel by Means of Resonant Cavities and Electrostatic Probes. Polytechnic Institute of Brooklyn, PIBAL Report No. 1019, May 1967.

7. Laframboise, Y.G.: Theory of Spherical and Cylindrical Langmuir Probes in a Collisionless Maxwellian Plasma at Rest. University of Toronto, Institute of Aerospace Studies, UTIAS Report No. 100, June 1966.

8. Sonin, A.A.: The Behavior of Free Molecule Cylindrical Langmuir Probes in Supersonic Flows and Their Application to the Study of the Blunt Body Stagnation Layer. University of Toronto, Institute of Aerospace Studies, UTIAS Report No. 109, August 1965.

9. Lederman, S., Bloom, M.H. and Widhopf, G.F.: Experiments in Cylindrical Electrostatic Probes in a Slightly Ionized Hypersonic Flow. AIAA J., 6, 11, pp. 2133-2139, November 1968.

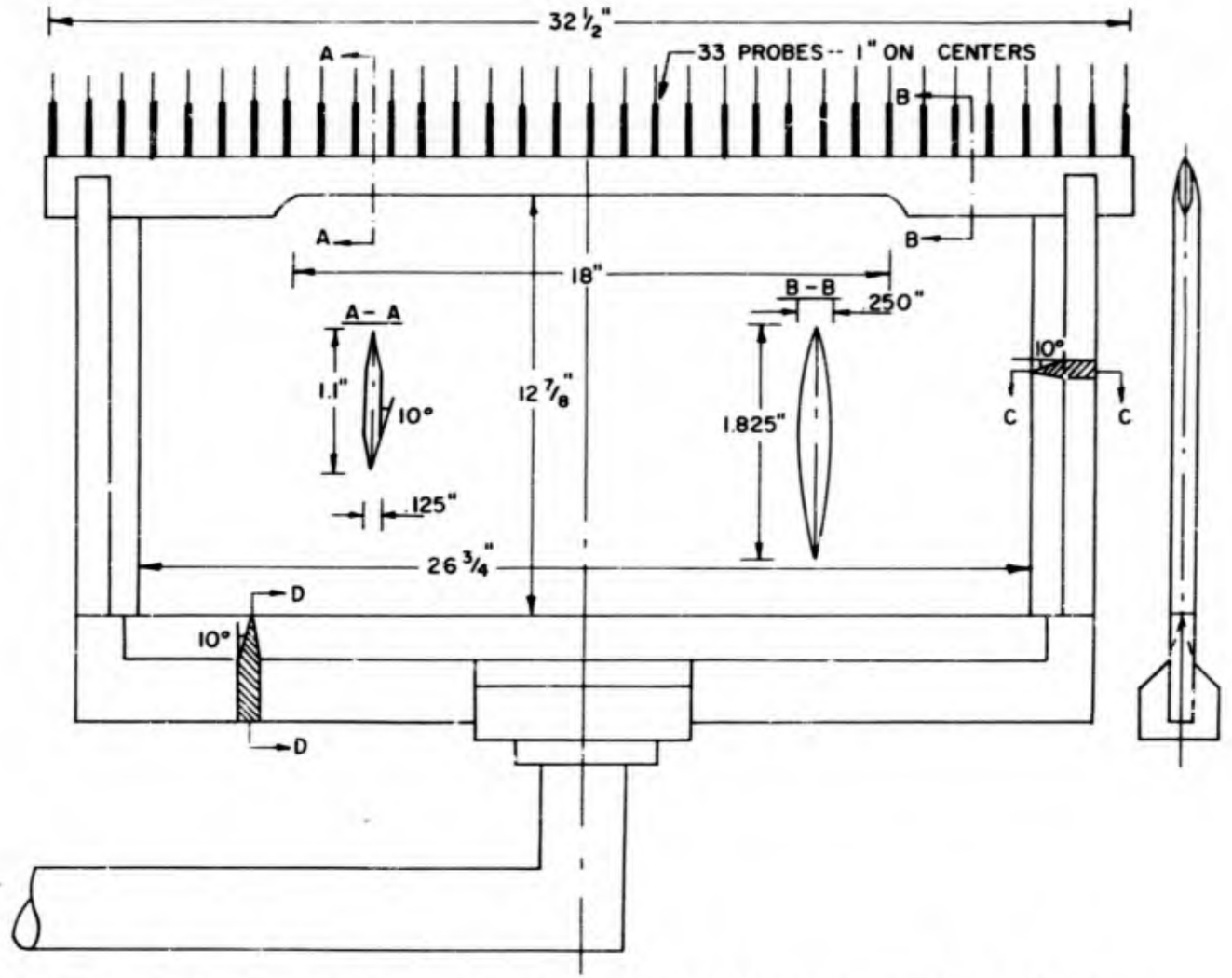

FIG. 1 SCHEMATIC DIAGRAM OF THE ELECTROSTATIC PROBE RAKE

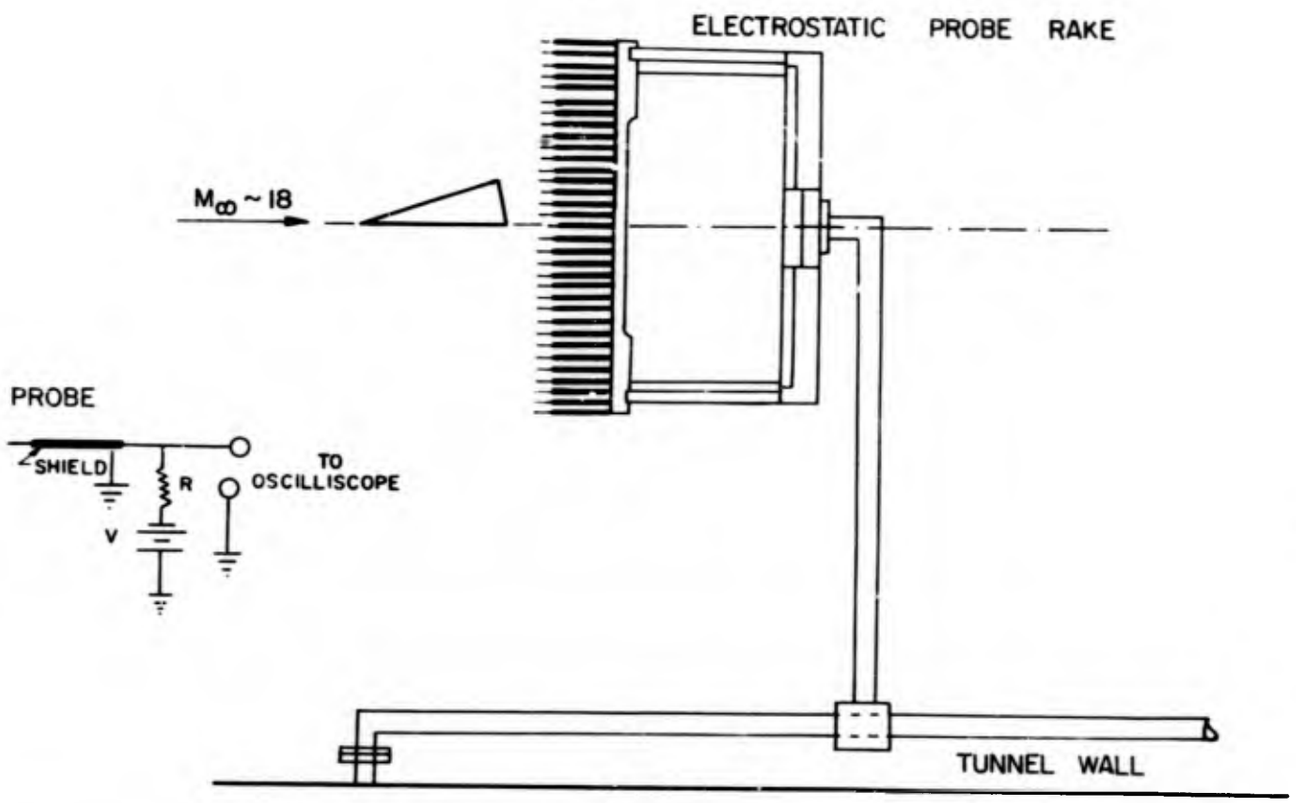

FIG. 2 SCHEMATIC DIAGRAM OF THE TEST CONFIGURATION FOR THE CONE AND THE ELECTROSTATIC PROBE CIRCUIT

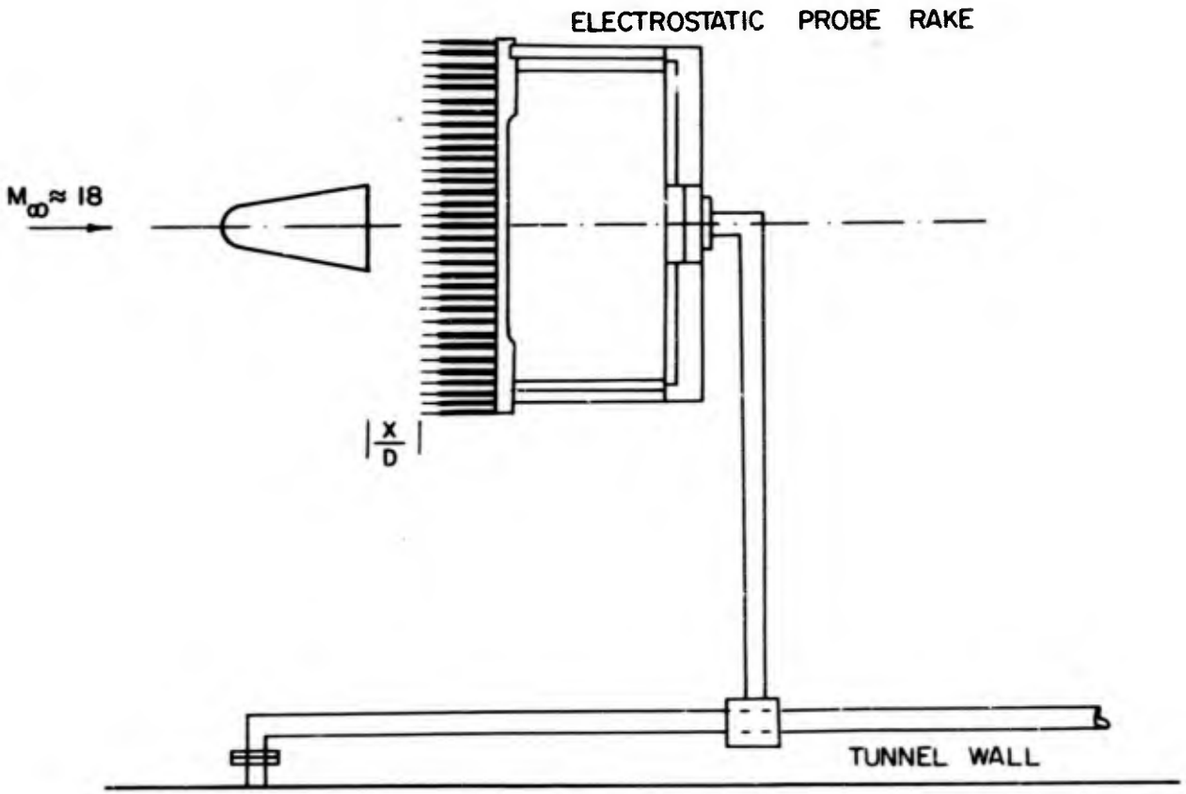

FIG. 2a SCHEMATIC DIAGRAM OF THE TEST CONFIGURATION FOR THE BLUNTED CONES

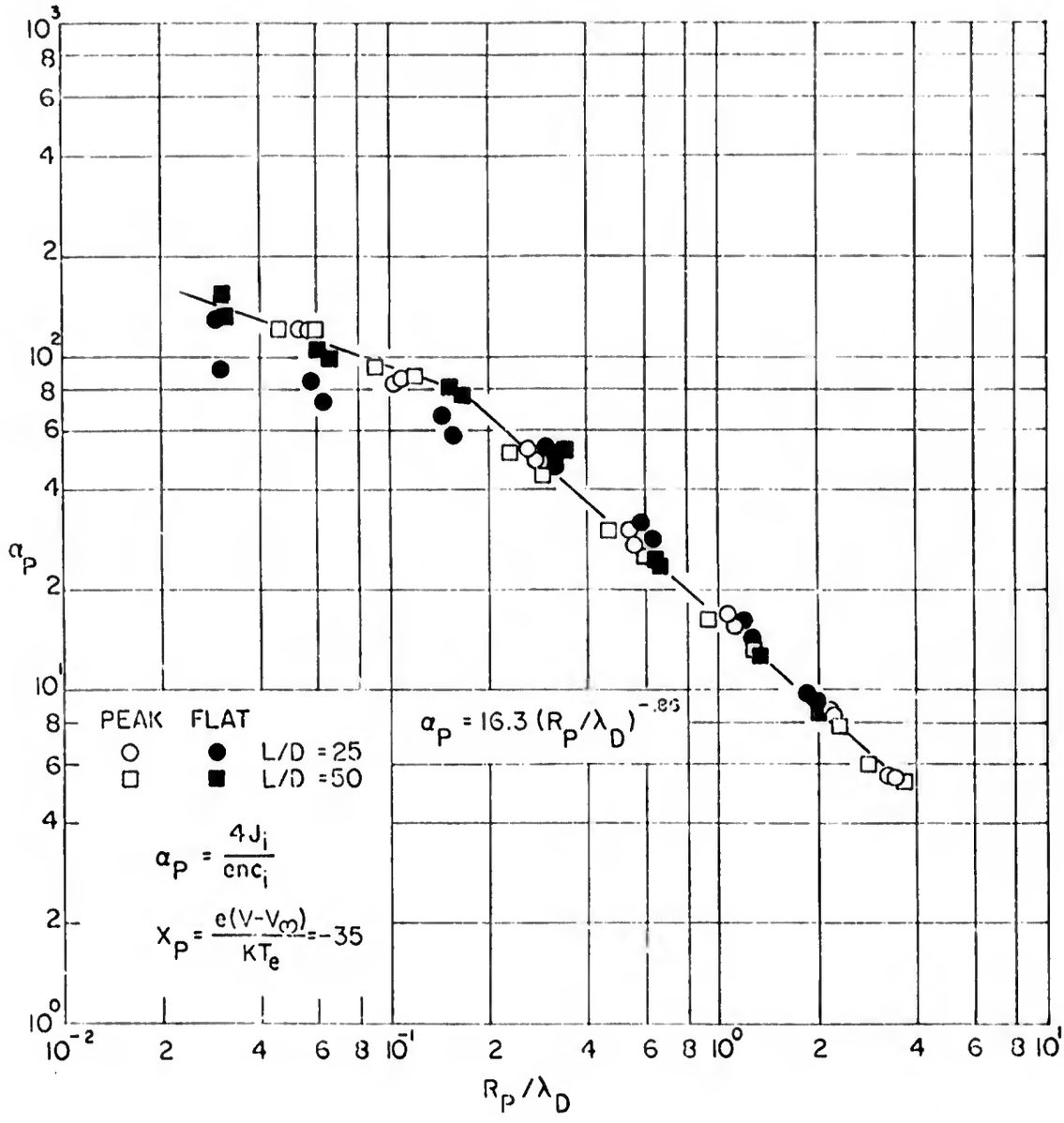

FIG. 3 NORMALIZED NONDIMENSIONAL ION CURRENT PARAMETER α_P AS A FUNCTION OF THE RATIO OF PROBE RADIUS TO DEBYE SHIELDING DISTANCE FOR $X_P = -35$

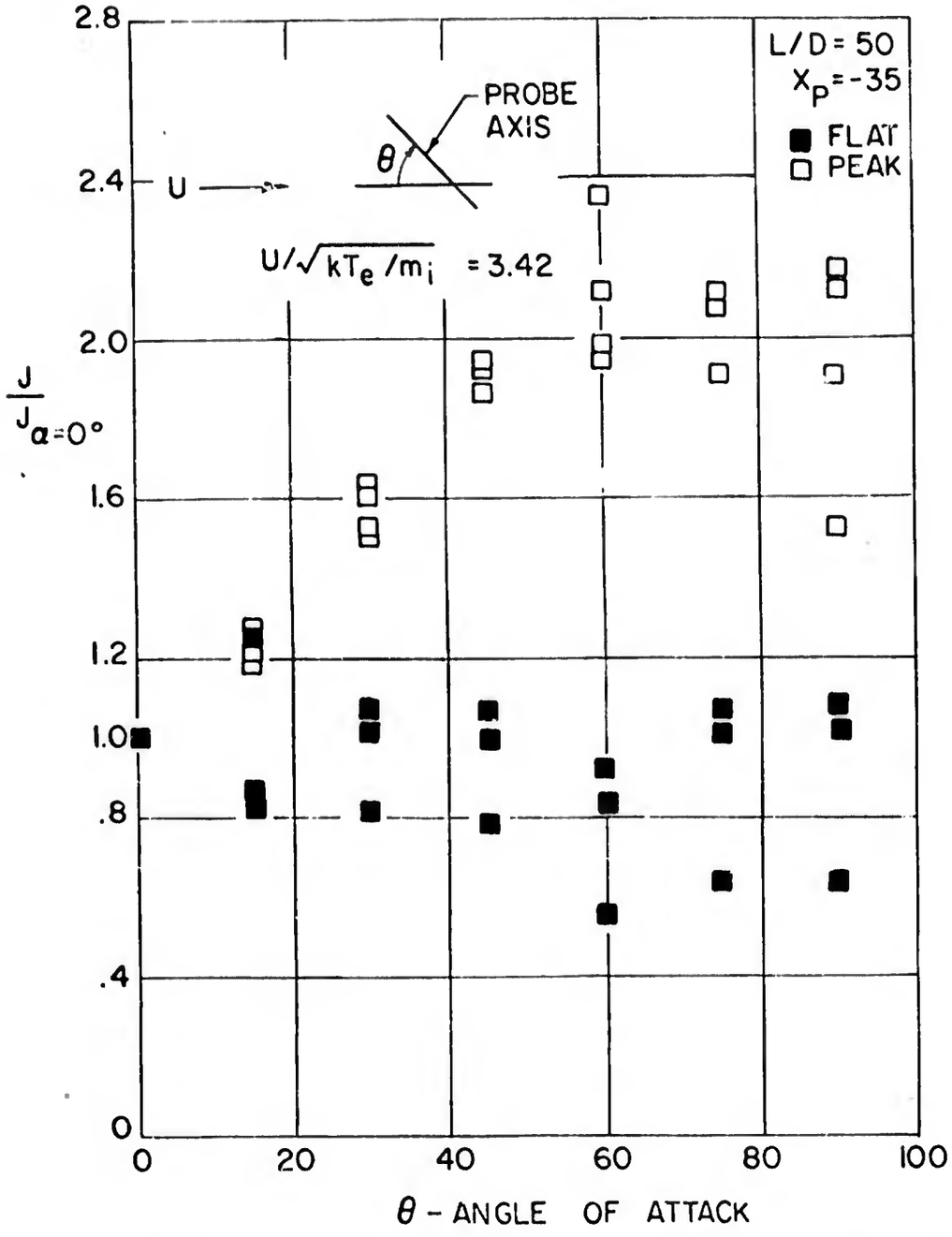

FIG. 4 NORMALIZED CURRENT DENSITY AS A FUNCTION OF PROBE ANGLE OF ATTACK

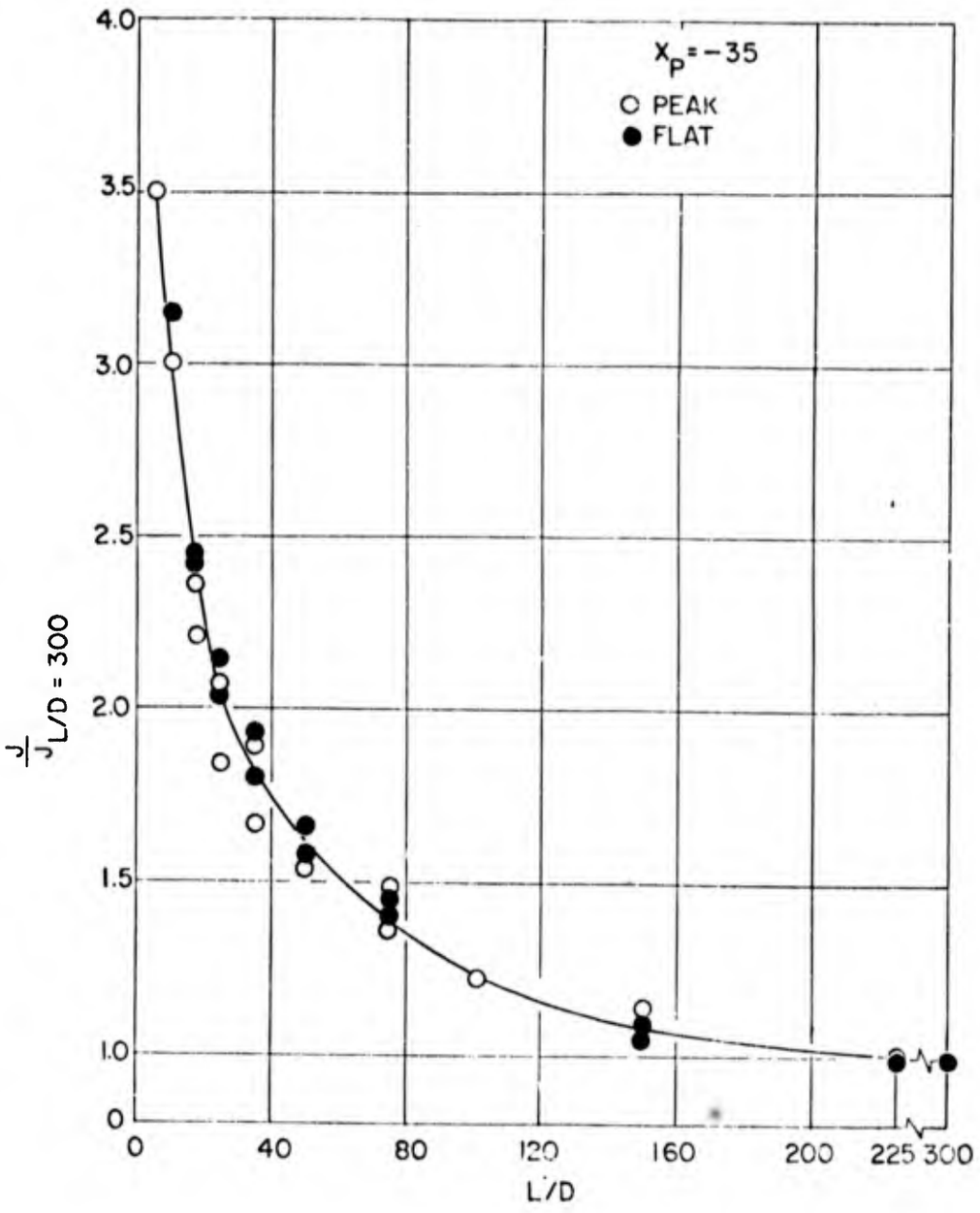

FIG. 5 NONDIMENSIONAL CURRENT DENSITY AS A FUNCTION OF THE PROBE LENGTH TO DIAMETER RATIO

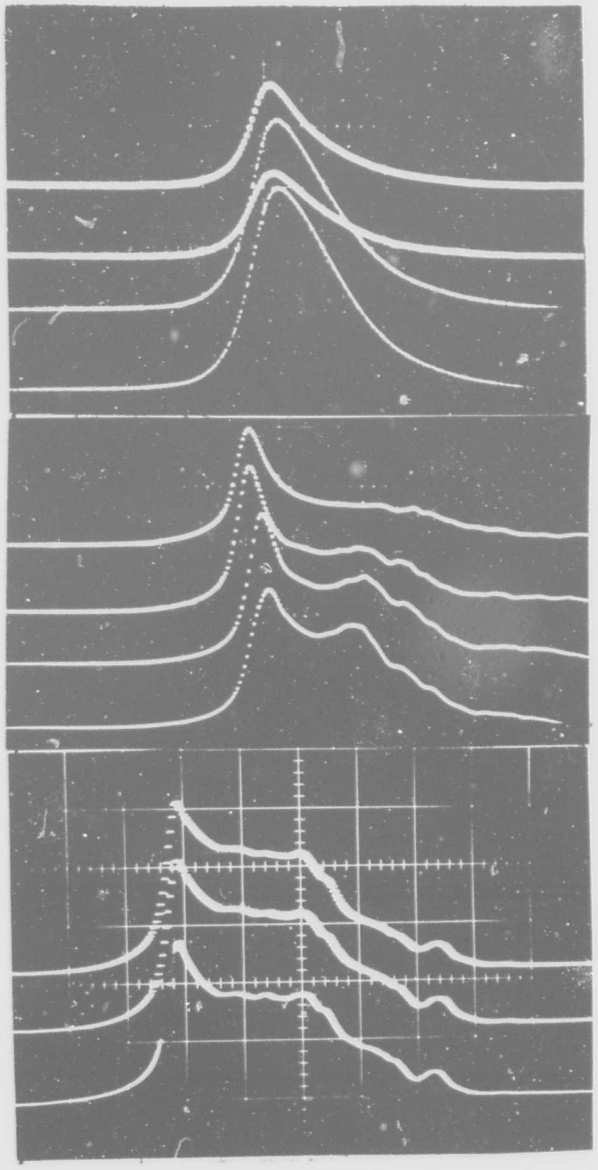

100 μ sec/Div.

FIG. 6 RESPONSES OF PROBES IN THE WAKE OF A 10° HALF ANGLE CONE. TOP TO BOTTOM TRACES REPRESENT CENTERLINE TO FREE STREAM RESPONSES

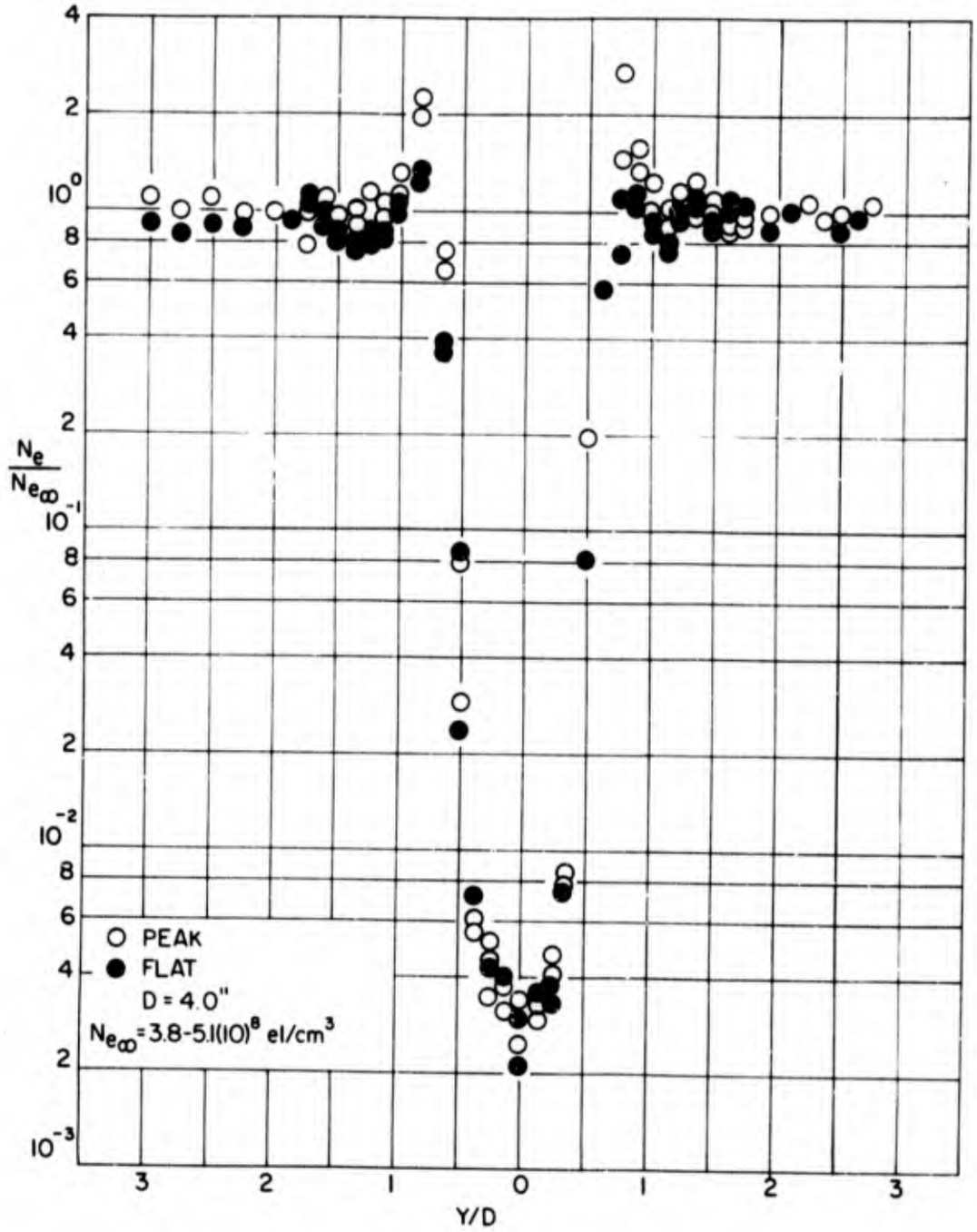

FIG. 7 NONDIMENSIONAL ELECTRON DENSITY DISTRIBUTION IN THE WAKE OF A CONE AT 0° ANGLE OF ATTACK AT X/D=0.25

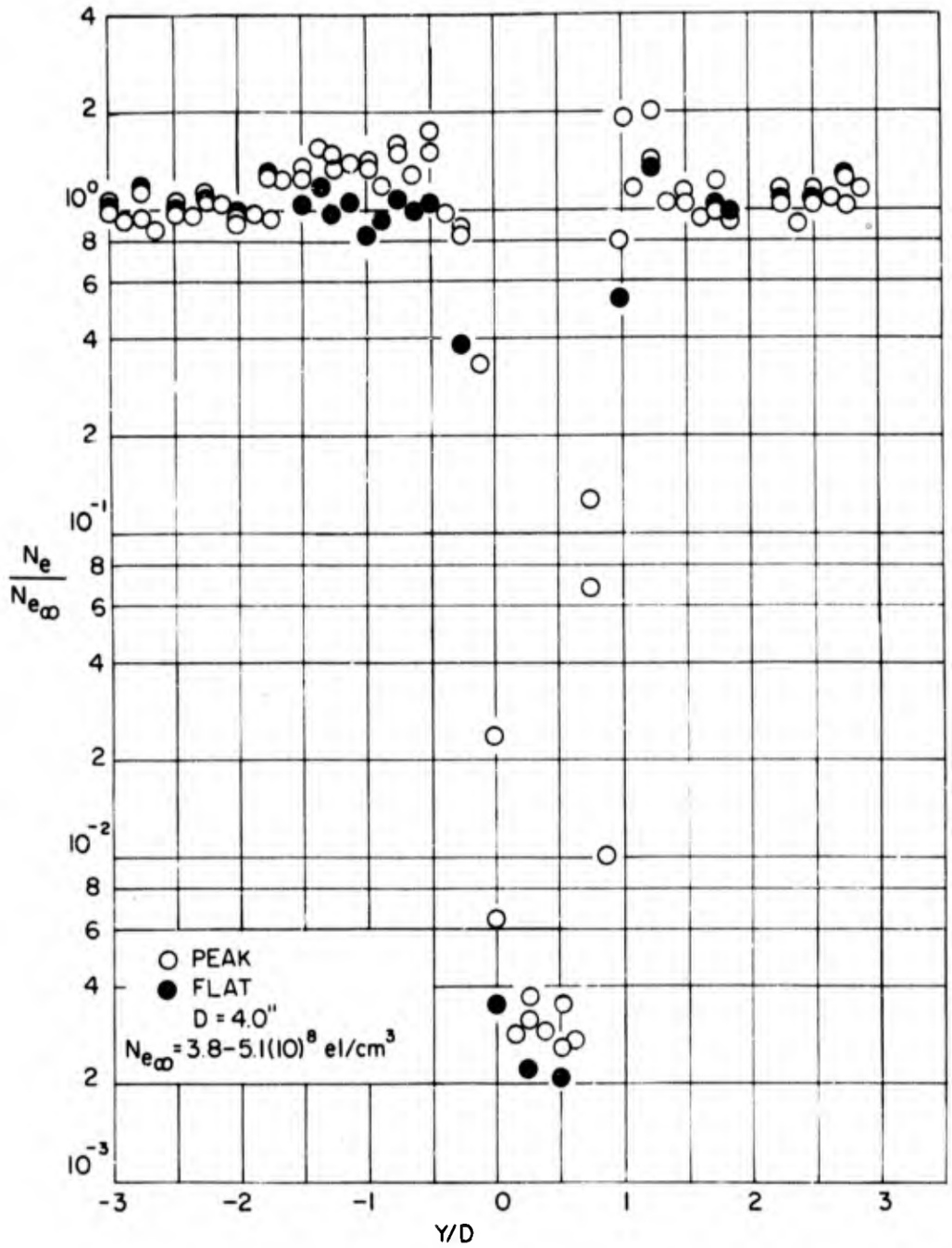

FIG. 8 NONDIMENSIONAL ELECTRON DENSITY DISTRIBUTION IN THE WAKE OF A 10° HALF ANGLE CONE AT 10° ANGLE OF ATTACK AT X/D = 0.25

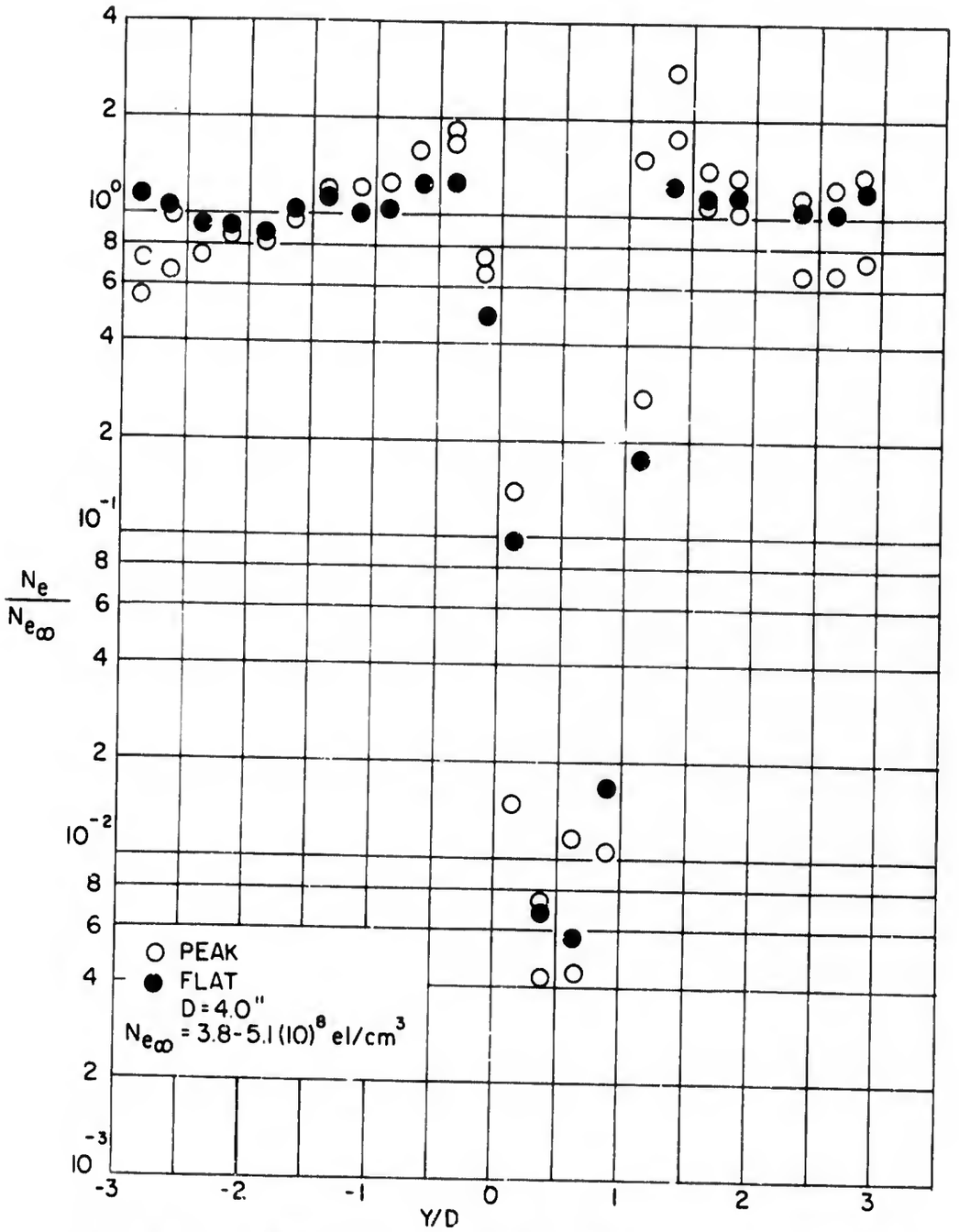

FIG. 9 NONDIMENSIONAL ELECTRON DENSITY DISTRIBUTION IN THE WAKE OF A 10° HALF ANGLE CONE AT 10° ANGLE OF ATTACK AT X/D = 0.50

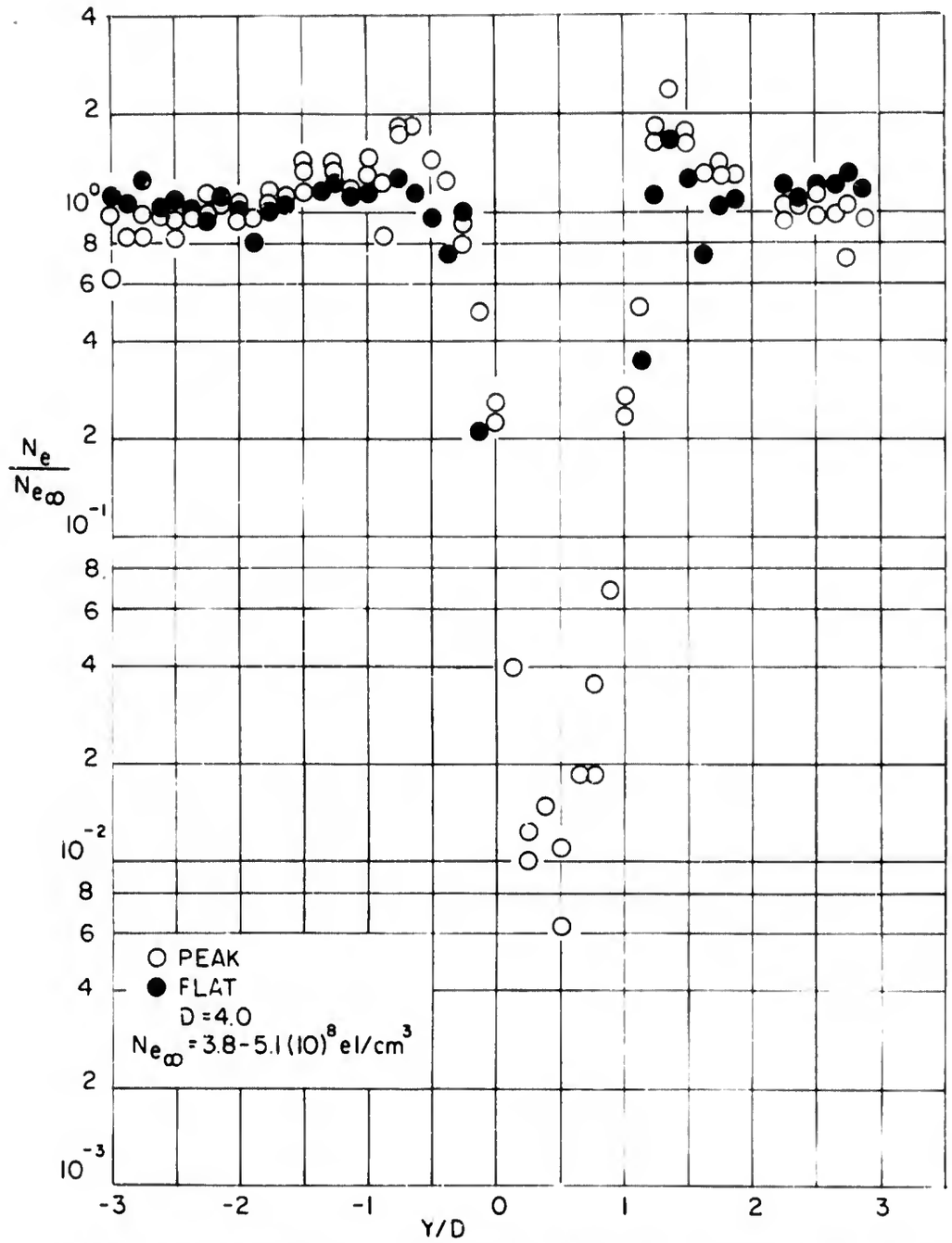

FIG. 10 NONDIMENSIONAL ELECTRON DENSITY DISTRIBUTION IN THE WAKE OF A 10° HALF ANGLE CONE AT 10° ANGLE OF ATTACK AT X/D = 0.75

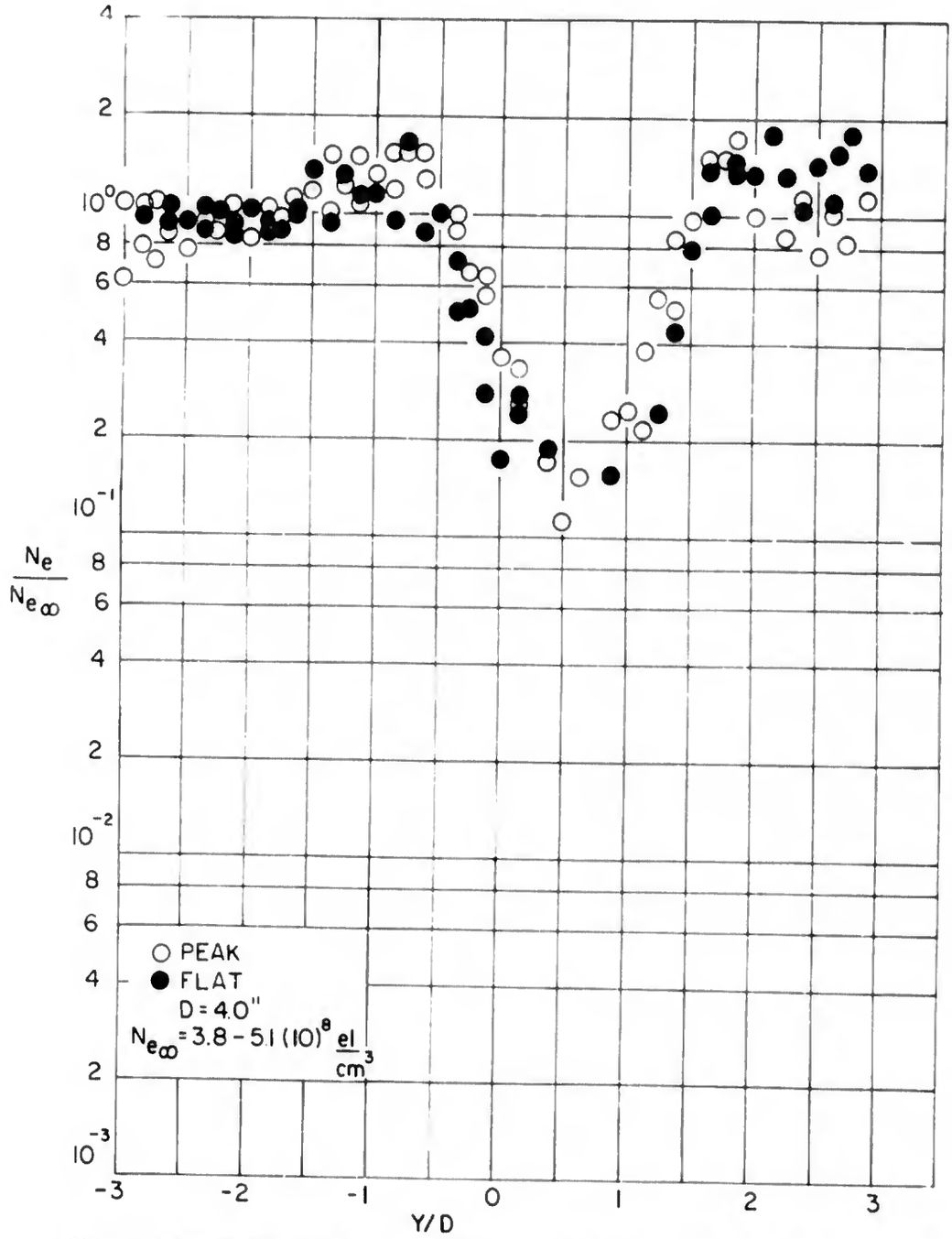

FIG 11 NONDIMENSIONAL ELECTRON DENSITY DISTRIBUTION IN THE WAKE OF A 10° HALF ANGLE CONE AT 10° ANGLE OF ATTACK AT X/D = 20

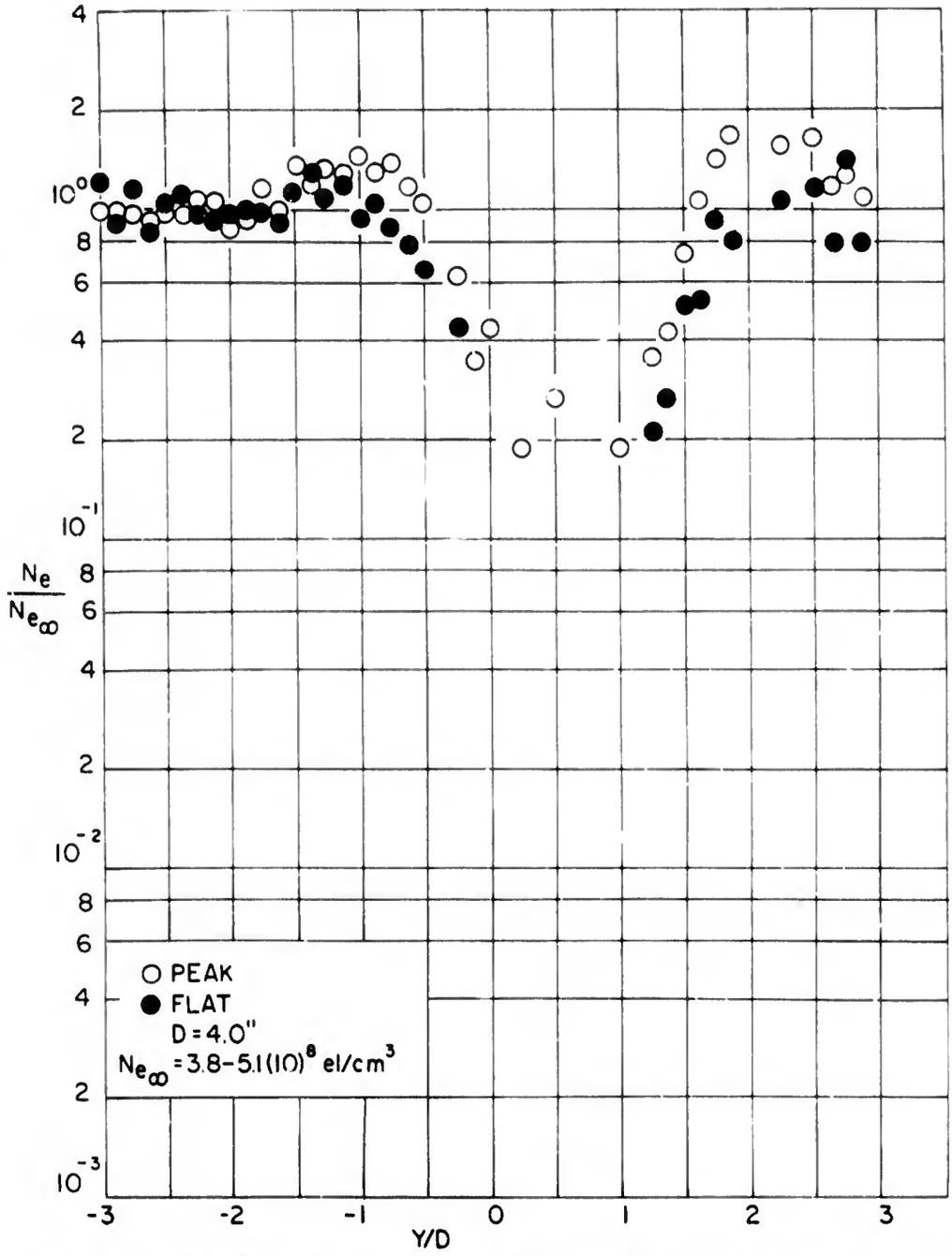

FIG. 12 NONDIMENSIONAL ELECTRON DENSITY DISTRIBUTION IN THE WAKE OF A 10° HALF ANGLE CONE AT 10° ANGLE OF ATTACK AT X/D = 3.0

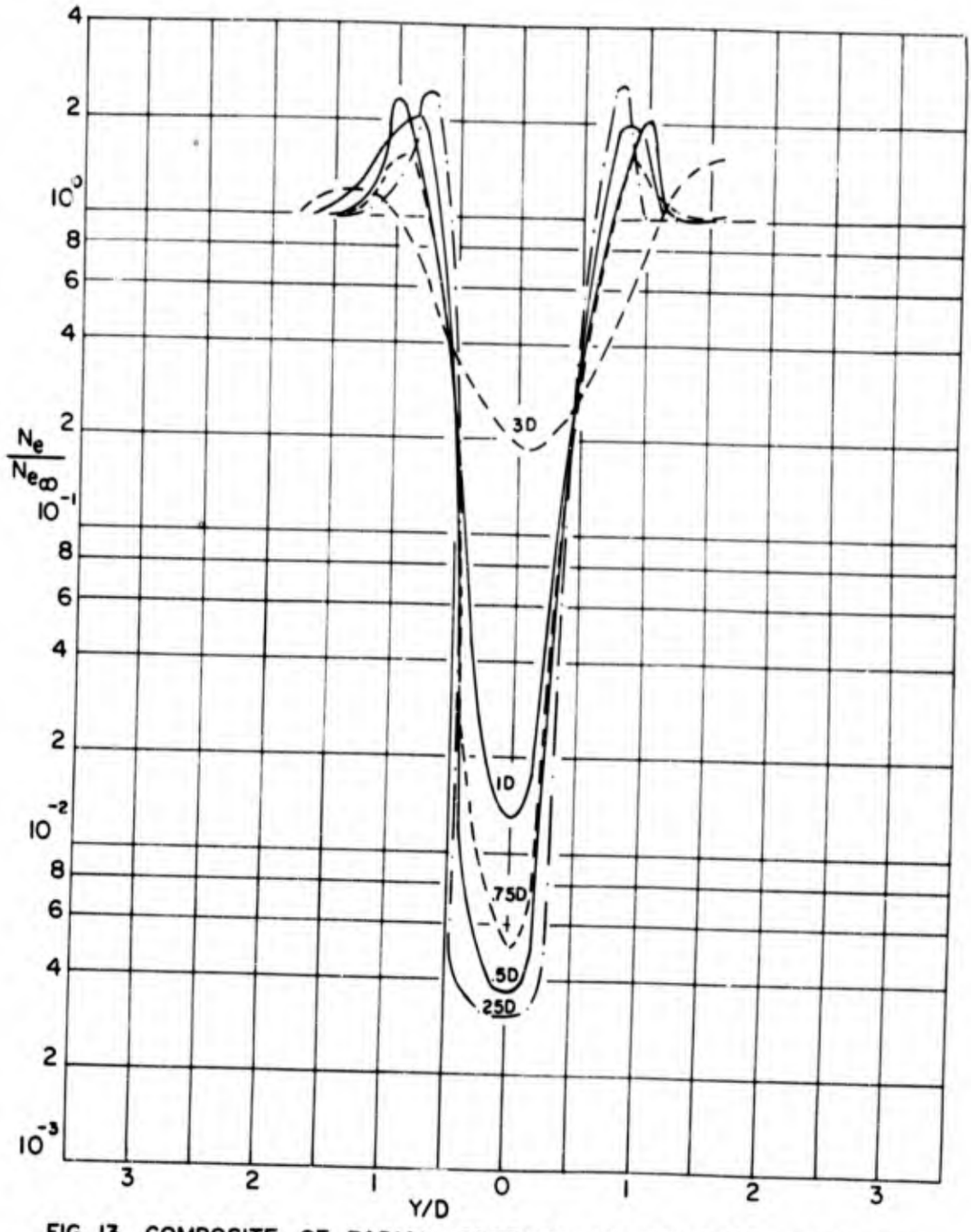

FIG. 13 COMPOSITE OF RADIAL PROFILES IN THE NEAR WAKE OF A 10° HALF ANGLE CONE AT VARIOUS AXIAL STATIONS AT 0° ANGLE OF ATTACK

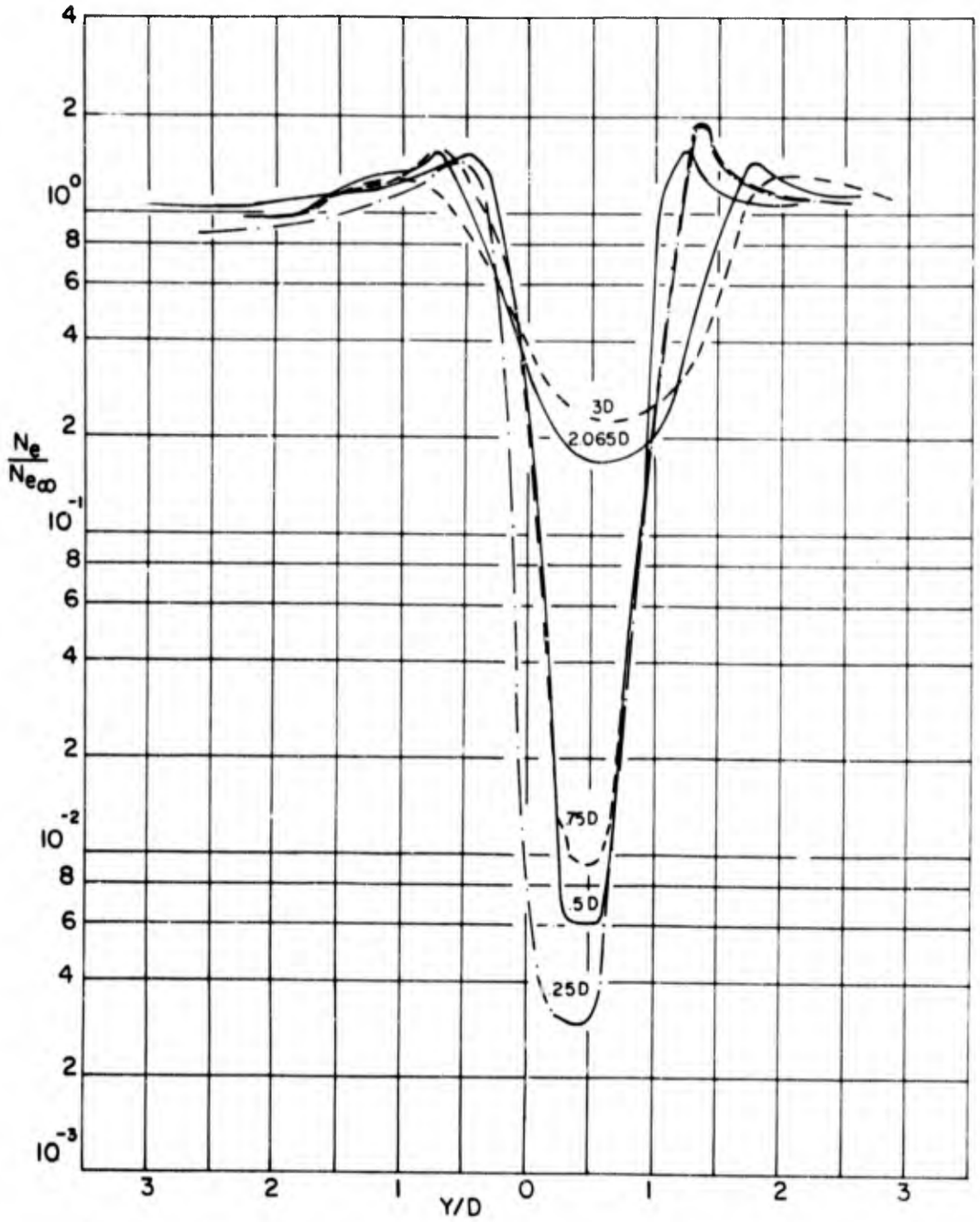

FIG. 14 COMPOSITE OF RADIAL PROFILES IN THE NEAR WAKE OF A 10° HALF ANGLE CONE AT VARIOUS AXIAL STATIONS AT 10° ANGLE OF ATTACK

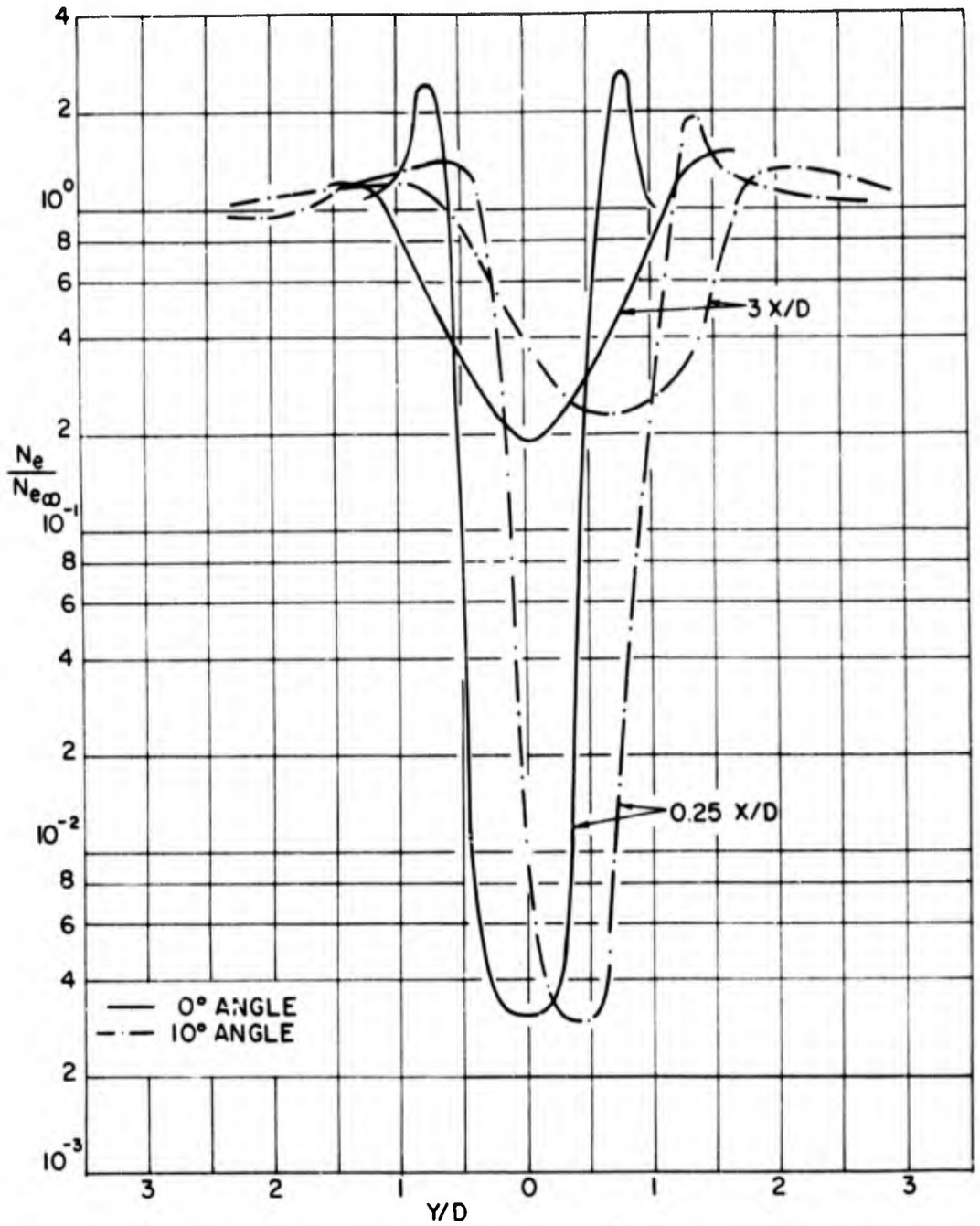

FIG. 15 COMPOSITE OF THE RADIAL DENSITY DISTRIBUTION IN THE WAKE OF A 10° HALF ANGLE CONE AT 0 AND 10° ANGLE OF ATTACK

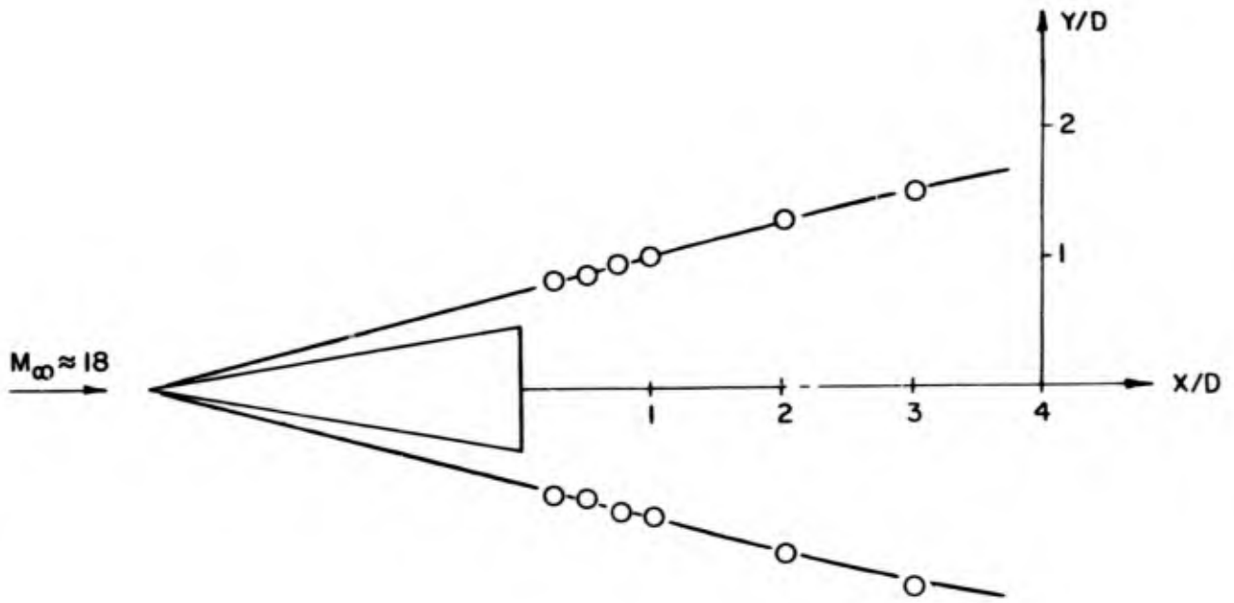

FIG. 15 EXPERIMENTAL SHOCK SHAPE FOR A 10° HALF ANGLE CONE AT 0° ANGLE OF ATTACK

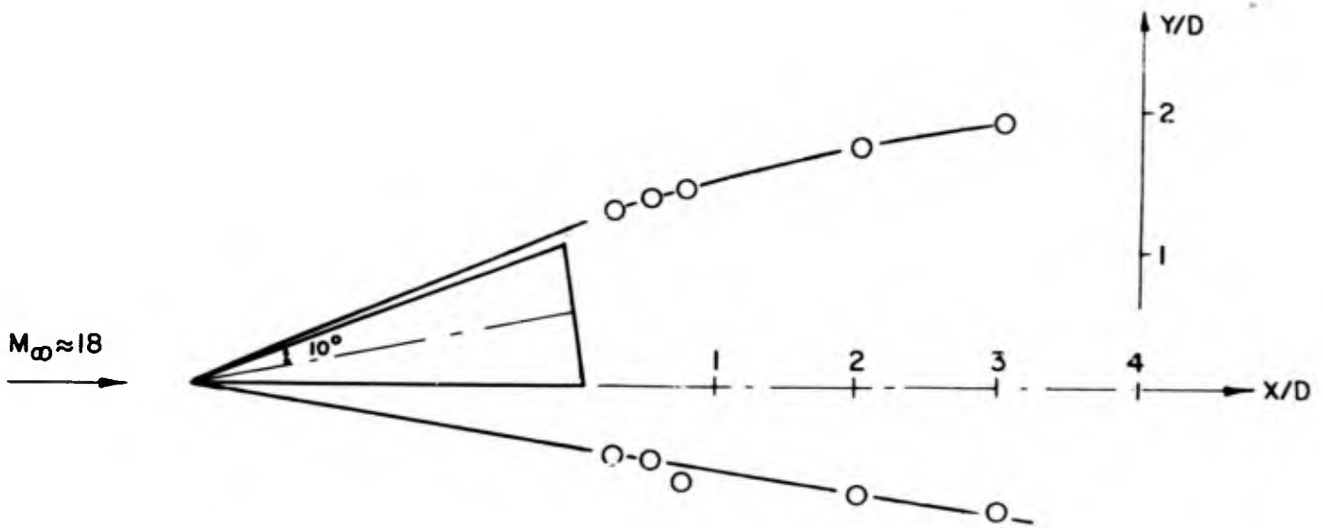

FIG. 17 EXPERIMENTAL SHOCK SHAPE FOR A 10° HALF ANGLE CONE AT 10° ANGLE OF ATTACK

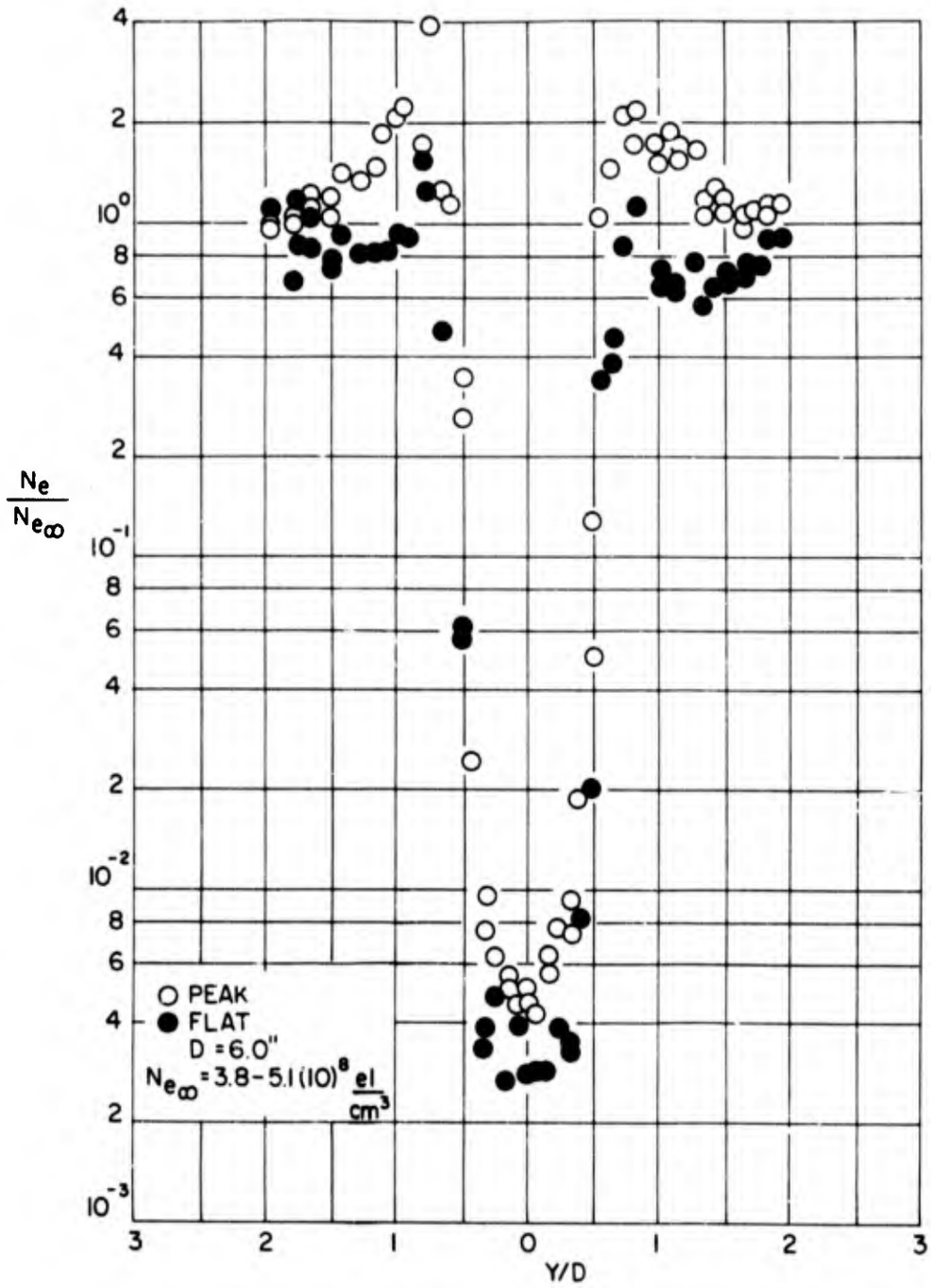

FIG. 18 NONDIMENSIONAL ELECTRON DENSITY DISTRIBUTION IN THE NEAR WAKE OF A 10° HALF ANGLE BLUNTED CONE B = 0.333, X/D = 0.25

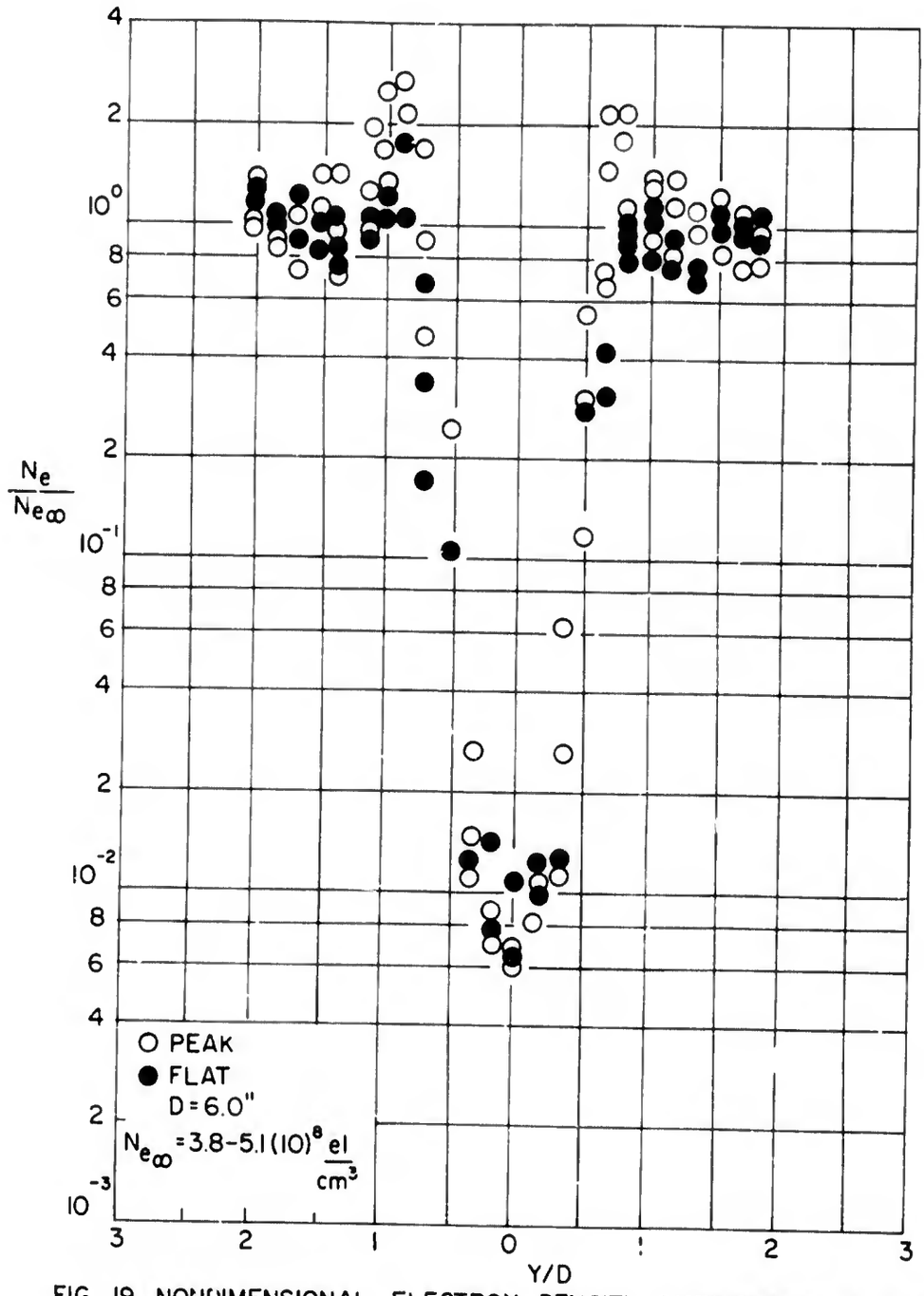

FIG. 19 NONDIMENSIONAL ELECTRON DENSITY DISTRIBUTION IN THE NEAR WAKE OF A 10° HALF ANGLE BLUNTED CONE B= 0.333, X/D = 0.5

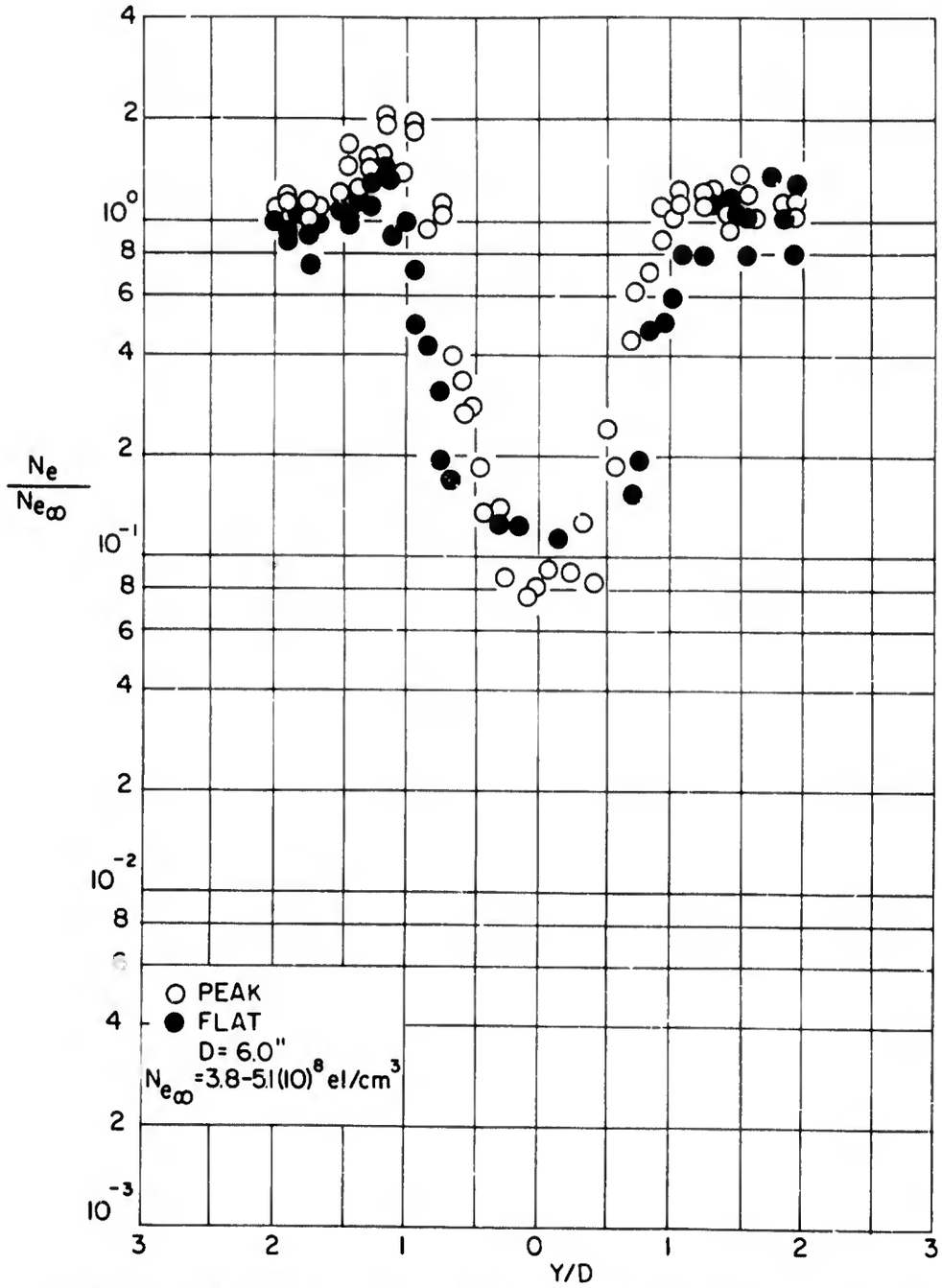

FIG. 20 NONDIMENSIONAL ELECTRON DENSITY DISTRIBUTION IN THE NEAR WAKE OF A 10° HALF ANGLE BLUNTED CONE B = 0.333, X/D=2.0

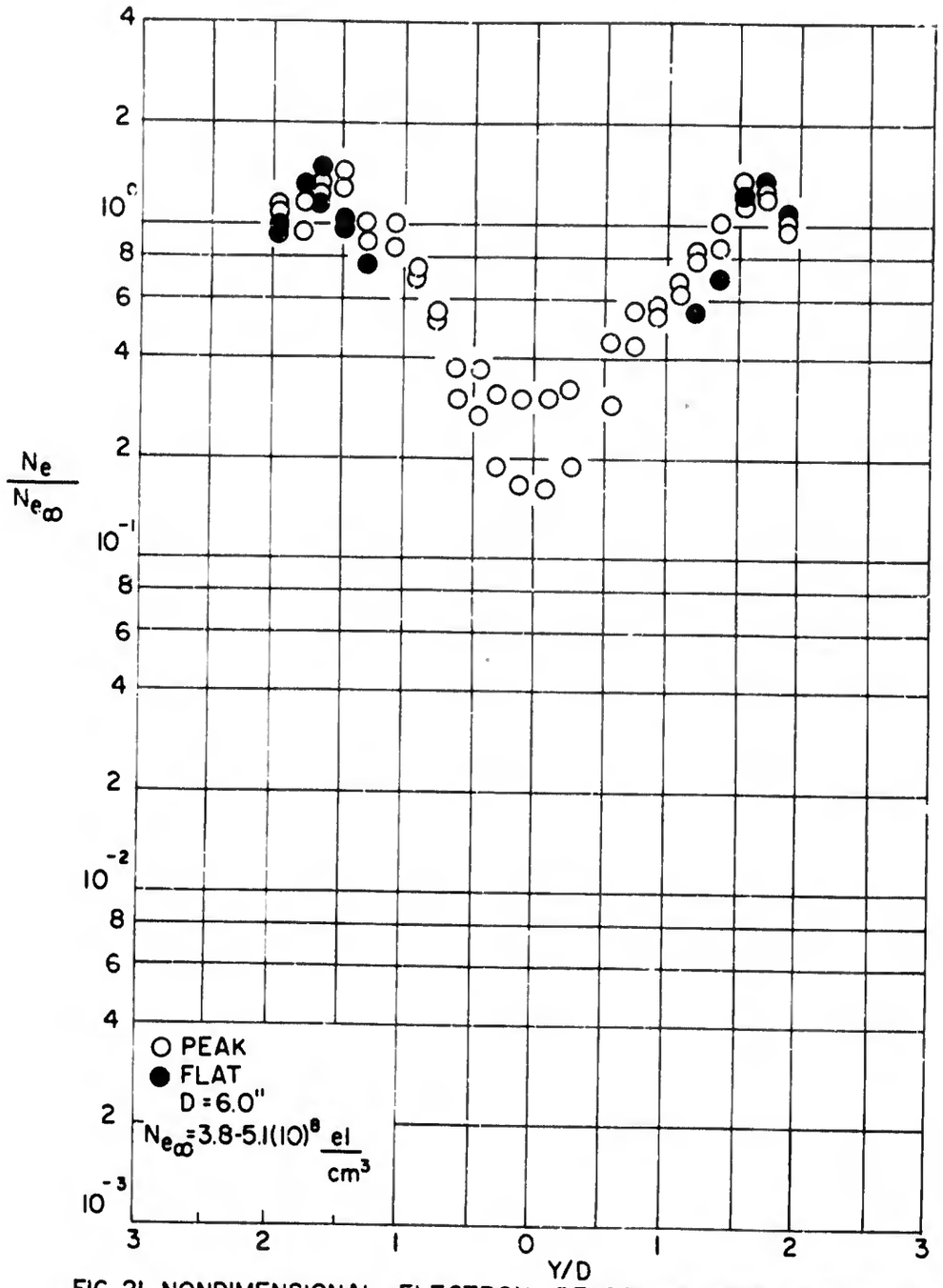

FIG. 21 NONDIMENSIONAL ELECTRON DENSITY DISTRIBUTION IN THE NEAR WAKE OF A 10° HALF ANGLE BLUNTED CONE B = 0.333, X/D = 4.0

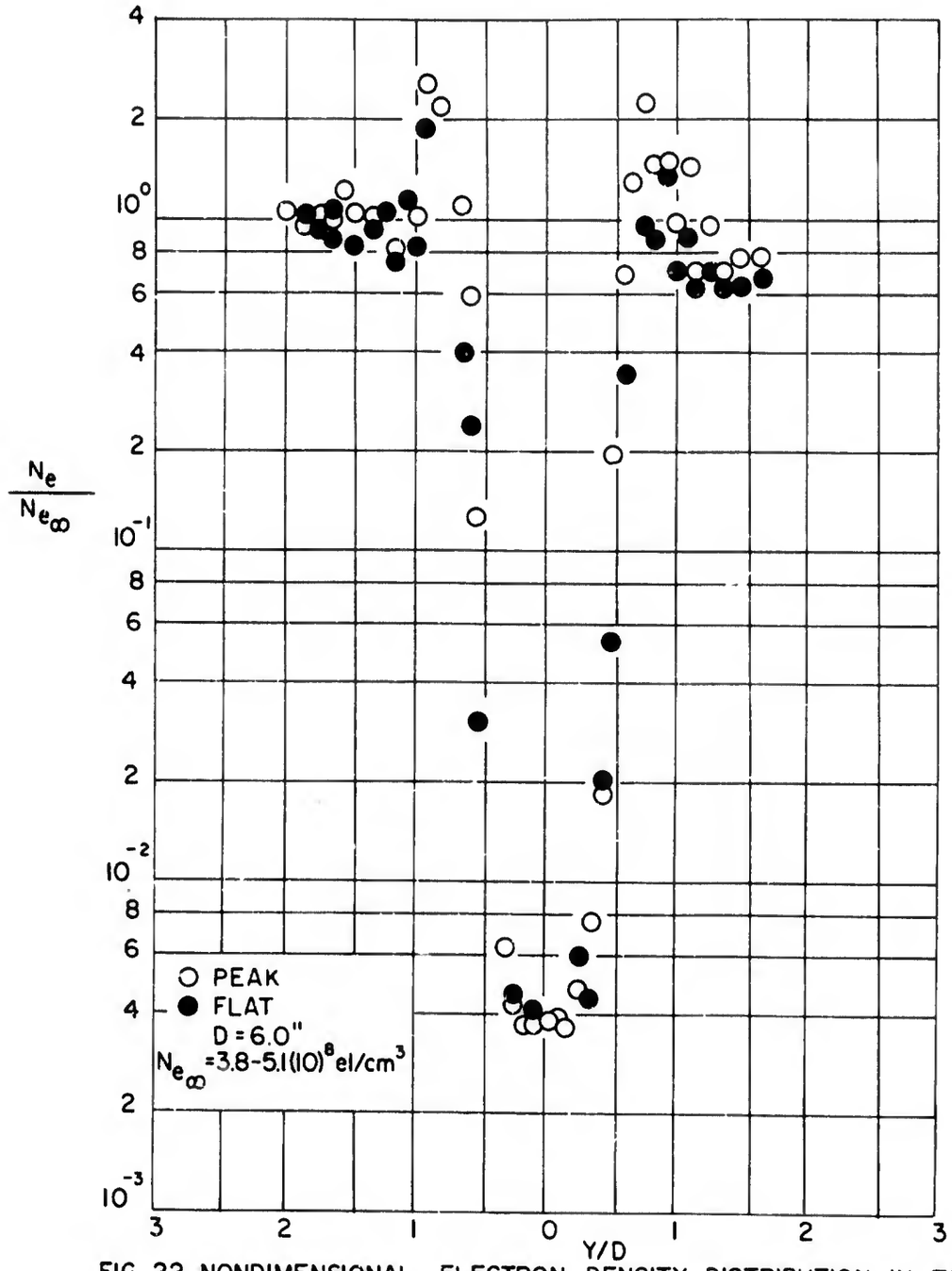

FIG. 22 NONDIMENSIONAL ELECTRON DENSITY DISTRIBUTION IN THE NEAR WAKE OF A 10° HALF ANGLE BLUNTED CONE B = 0.666, X/D = 0.25

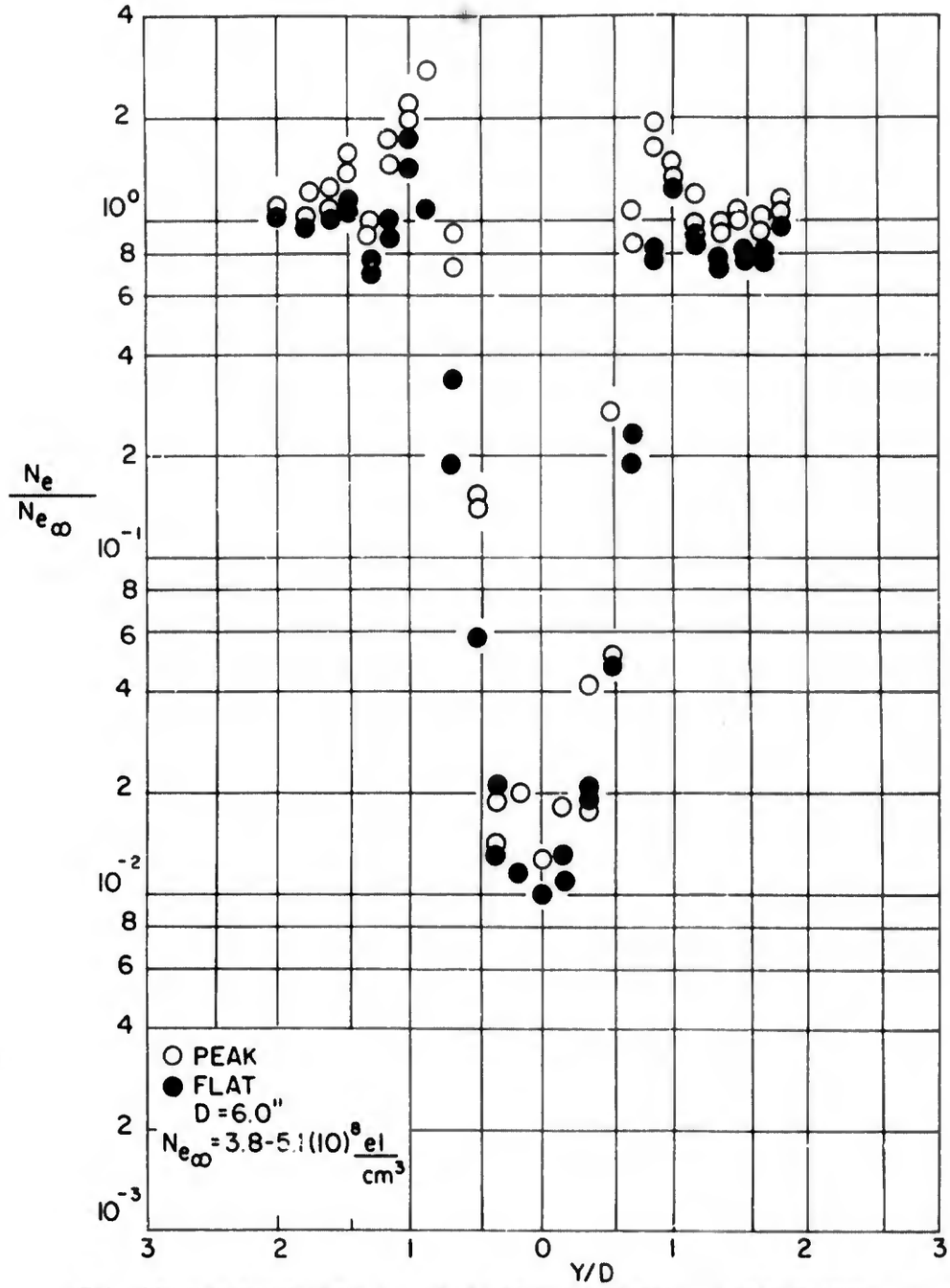

FIG. 23 NONDIMENSIONAL ELECTRON DENSITY DISTRIBUTION IN THE NEAR WAKE OF A 10° HALF ANGLE BLUNTED CONE B = 0.666, X/D = 0.50

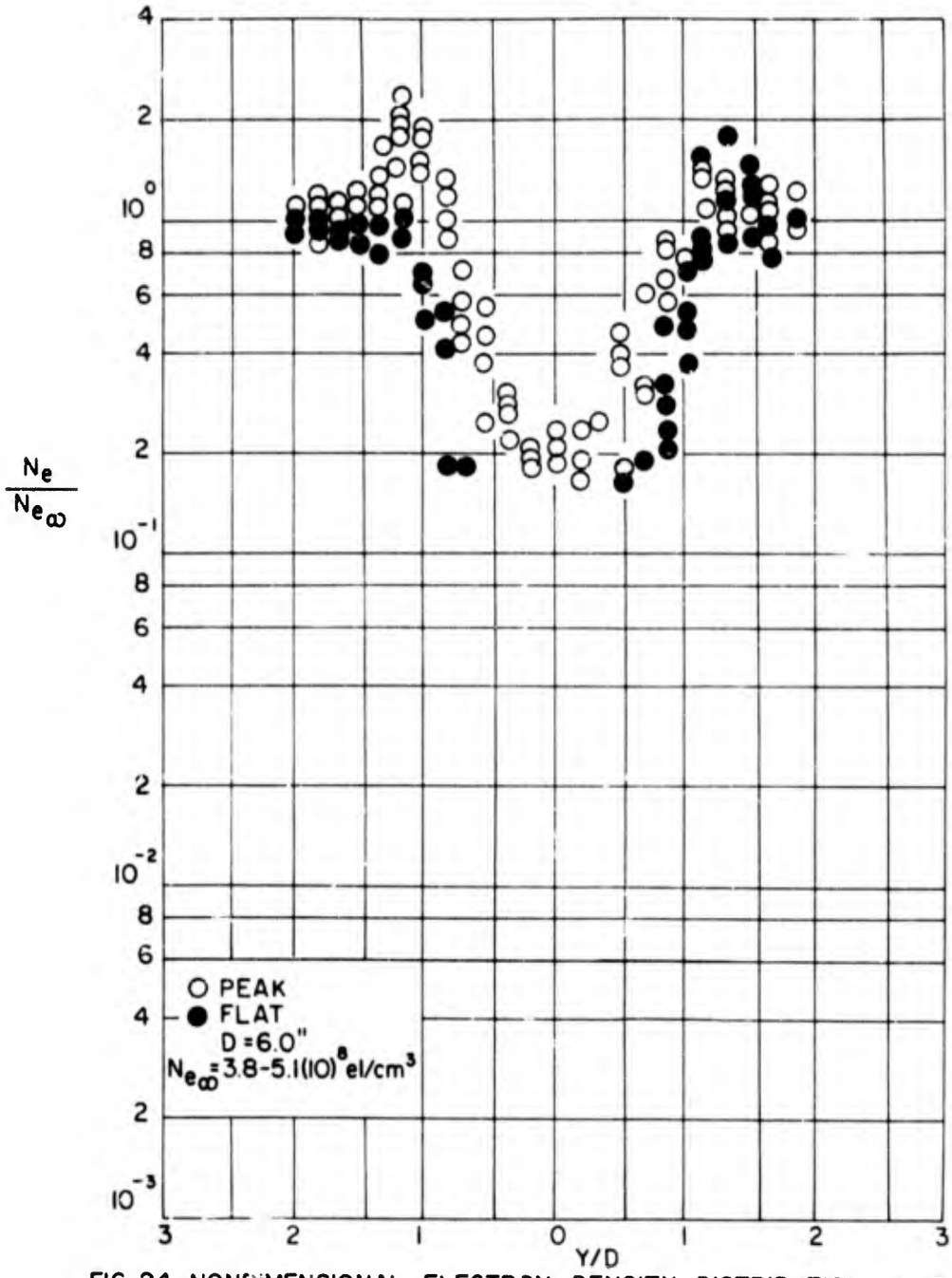

FIG. 24 NONDIMENSIONAL ELECTRON DENSITY DISTRIBUTION IN THE NEAR WAKE OF A 10° HALF ANGLE BLUNTED CONE B = 0.666, X/D = 2.0

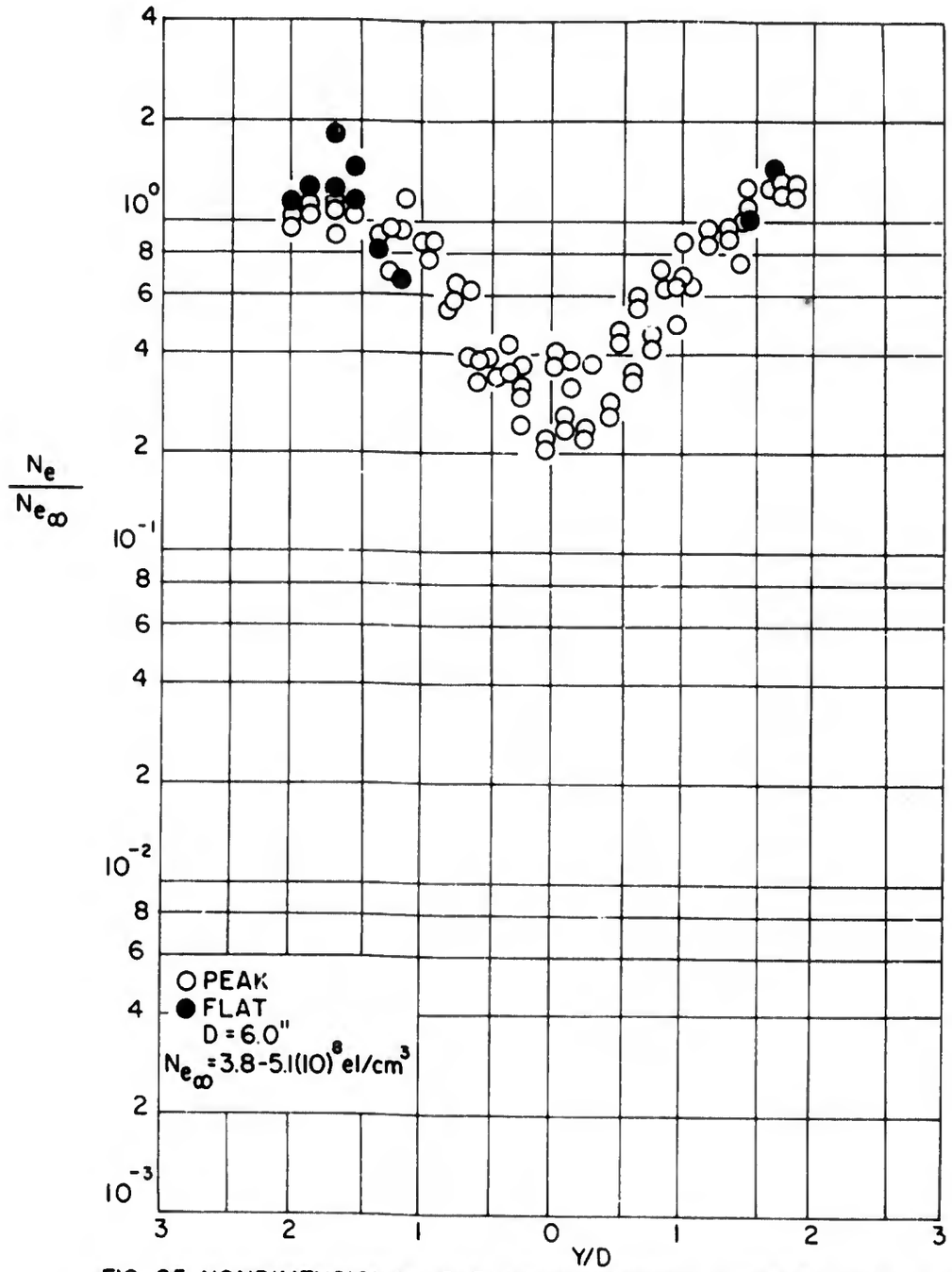

FIG. 25 NONDIMENSIONAL ELECTRON DENSITY DISTRIBUTION IN THE NEAR WAKE OF A 10° HALF ANGLE BLUNTED CONE B = 0.666, X/D = 4.0

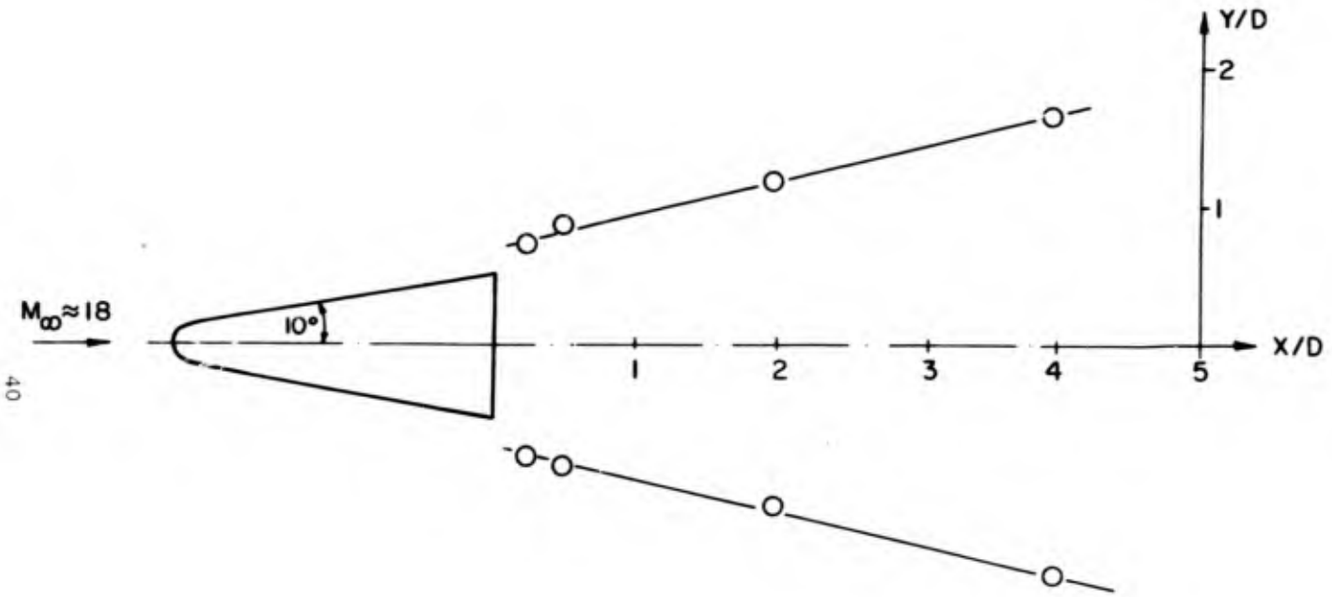

FIG. 26 EXPERIMENTAL SHOCK SHAPE FOR A 10° HALF ANGLE BLUNTED CONE (B = 0.333) AT 0° ANGLE OF ATTACK

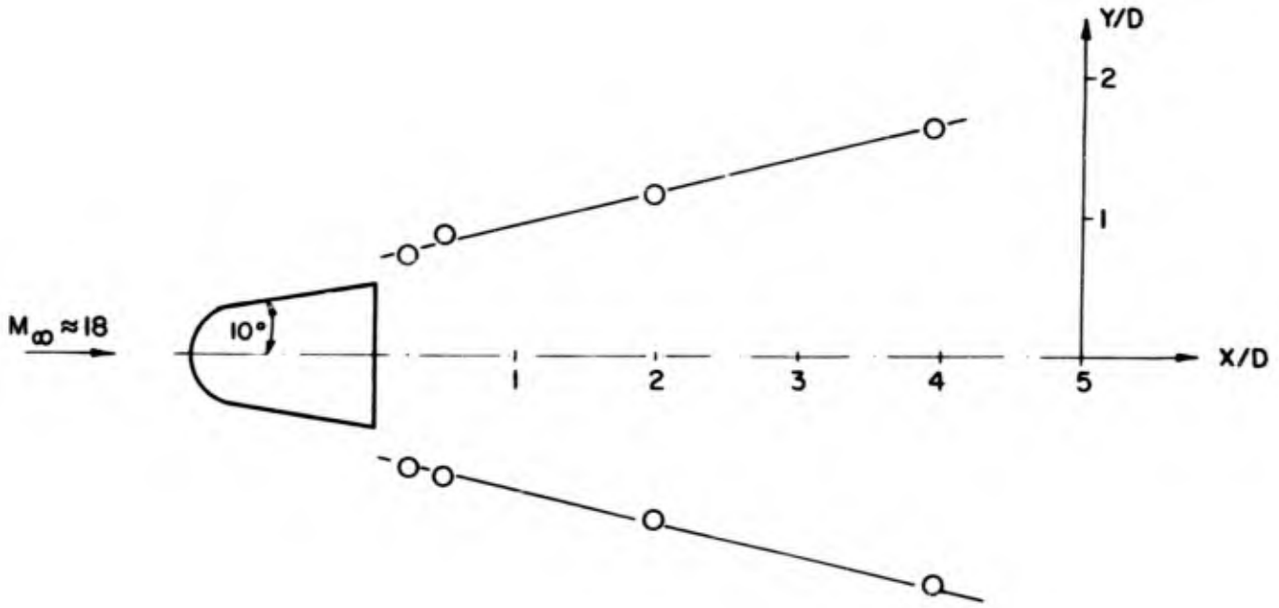

FIG. 27 EXPERIMENTAL SHOCK SHAPE FOR A 10° HALF ANGLE BLUNTED CONE (B = 0.666) AT 0° ANGLE OF ATTACK

Unclassified
Security Classification

DOCUMENT CONTROL DATA - P & D
(Security classification of title, body of abstract and indexing annotation must be entered when the overall report is classified)

1 ORIGINATING ACTIVITY (Corporate author)
Polytechnic Institute of Brooklyn
Dept. of Aerospace Engrg. & Applied Mechanics
Route 110, Farmingdale, N.Y. 11735

2a. REPORT SECURITY CLASSIFICATION
Unclassified

2b. GROUP

3 REPORT TITLE
EXPERIMENTAL MEASUREMENTS IN THE WAKE OF 10° HALF ANGLE BLUNTED AND POINTED CONES AT HYPERSONIC FLOW VELOCITIES

4 DESCRIPTIVE NOTES (Type of report and inclusive dates)
Research report

5 AUTHOR(S) (First name, middle initial, last name)
Samuel Lederman
Joel Avidor

6 REPORT DATE
May 1969

7a. TOTAL NO OF PAGES
41

7b. NO. OF REFS
9

8a. CONTRACT OR GRANT NO
Nonr 839(38)

b. PROJECT NO

c. ARPA Order No. 529

d.

9a. ORIGINATOR'S REPORT NUMBER(S)
PIBAL Report No. 69-15

9b. OTHER REPORT NO(S) (Any other numbers that may be assigned this report)

10 DISTRIBUTION STATEMENT
Distribution of this document is unlimited.

11 SUPPLEMENTARY NOTES

12 SPONSORING MILITARY ACTIVITY
Office of Naval Research
Electronics Branch
Washington, D.C. 20360

13 ABSTRACT

Experimental measurements have been performed in the wake of a 10° half angle cone at 0° and 10° angle of attack with respect to the flow, and of a blunted cone of .333, and .666 bluntness ratio at 0° angle of attack. A rake of closely spaced (1" apart) electrostatic probes was utilized to obtain the relative electron density distribution at several stations behind the base of the cone. These electron densities can, under certain conditions and in most parts of the wake, be interpreted in terms of the neutral density distributions. It is concluded that the hypersonic shock tunnel in conjunction with simple electrostatic probes can, within limits, provide a good qualitative insight into the flow field of complex aerodynamic models.

DD FORM 1 NOV 65 1473

Unclassified
Security Classification

14 KEY WORDS	LINK A		LINK B		LINK C	
	ROLE	WT	ROLE	WT	ROLE	WT
Fluid dynamics						
Near wake						
Electron density distribution						
Biased electrostatic probes						
Hypersonic flow						
Shock wave						
Blunted cone						
Pointed cone						